Photonuclear Dijet Production in Ultra-Peripheral Pb+Pb Collisions at 5.02 TeV with the ATLAS Detector

Ben Gilbert
On behalf of the ATLAS Collaboration

ATLAS-HION-2022-15 (arXiv:2409.11060)

Photonuclear Jet Production

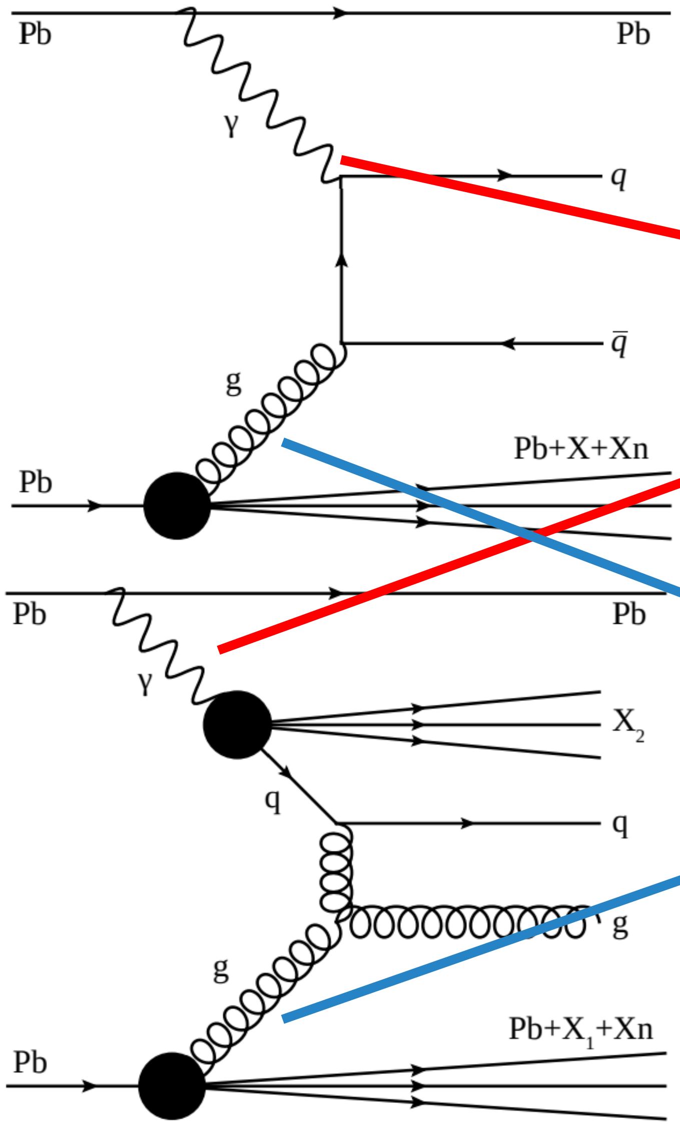

In ultra-relativistic heavy ion collisions, the intense electromagnetic fields provide an intense flux of nearly real photons.

Emitted photons may strike a parton in the other nucleus.

Photonuclear Jet Production

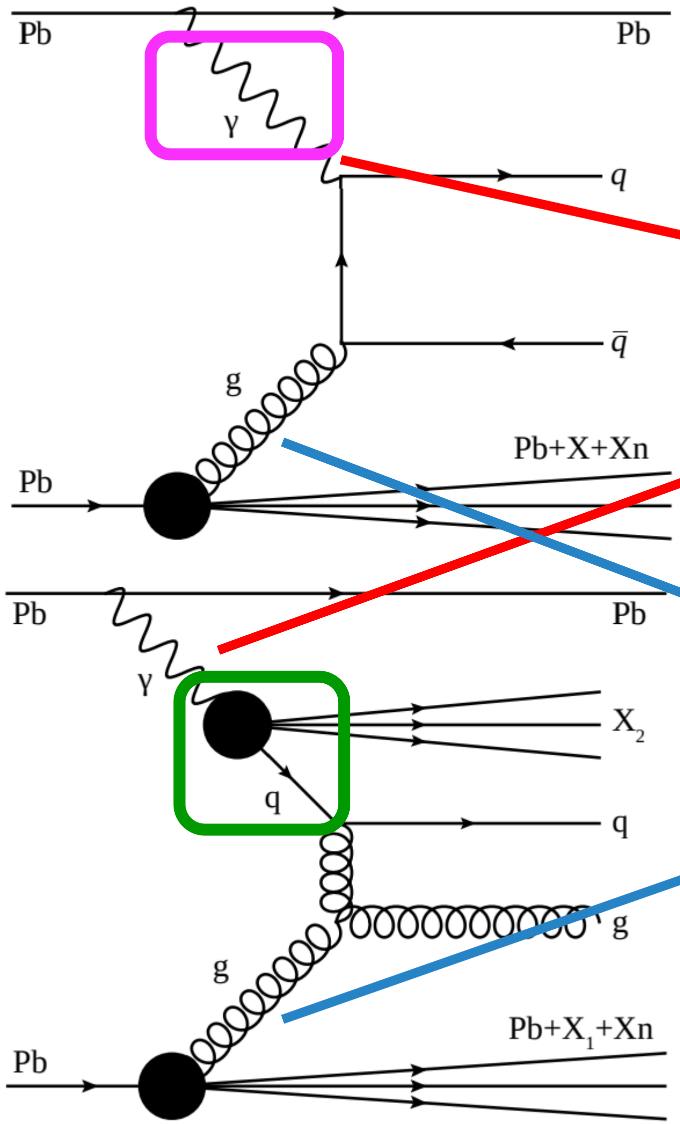

In ultra-relativistic heavy ion collisions, the intense electromagnetic fields provide an intense flux of nearly real photons.

"Direct" photons participate in the hard-scattering process.

"Resolved" photons scatter through a virtual hadronic excitation of the photon.

Emitted photons may strike a parton in the other nucleus.

Sensitivity to nPDF Effects

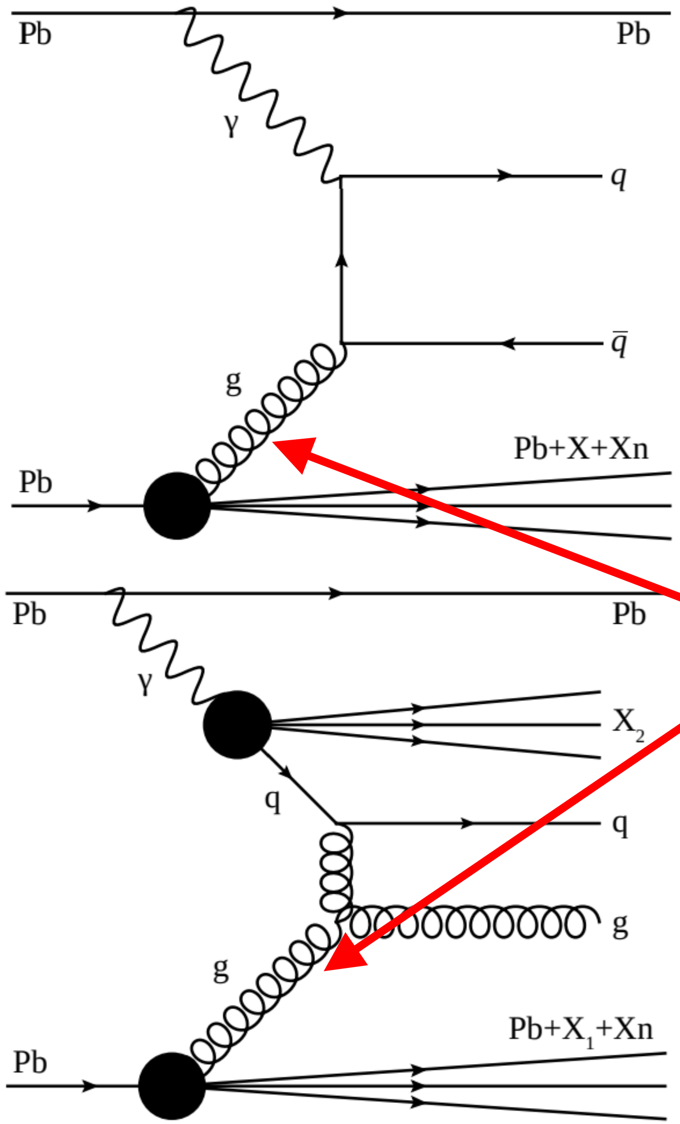

Jets provide access to the full hard-scattering kinematics!

Photonuclear jet measurements can access the nPDFs of struck ions in a kinematic region with little available data.

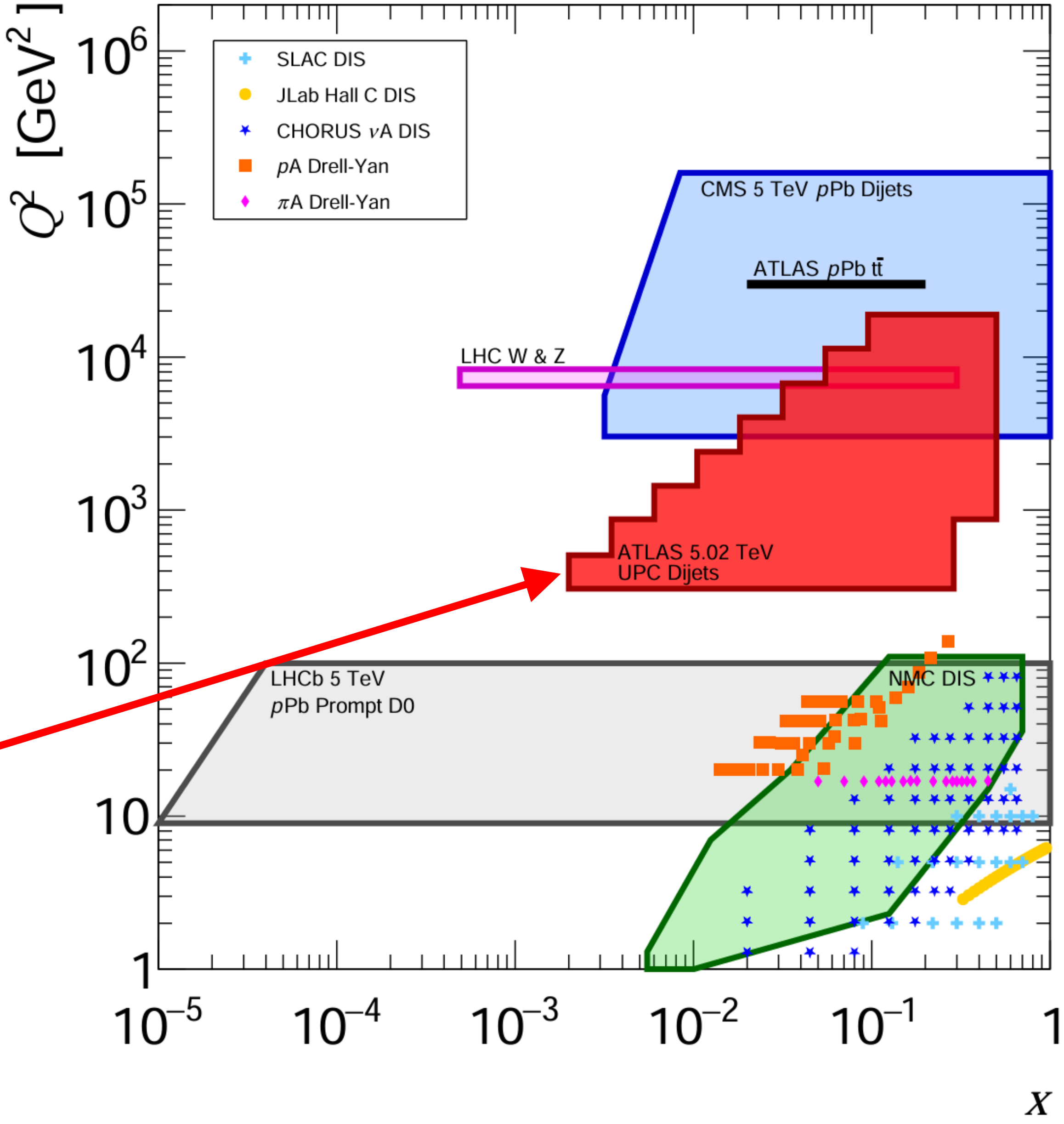

Figure inspired by arXiv:2112.12462

Photonuclear Jet Production

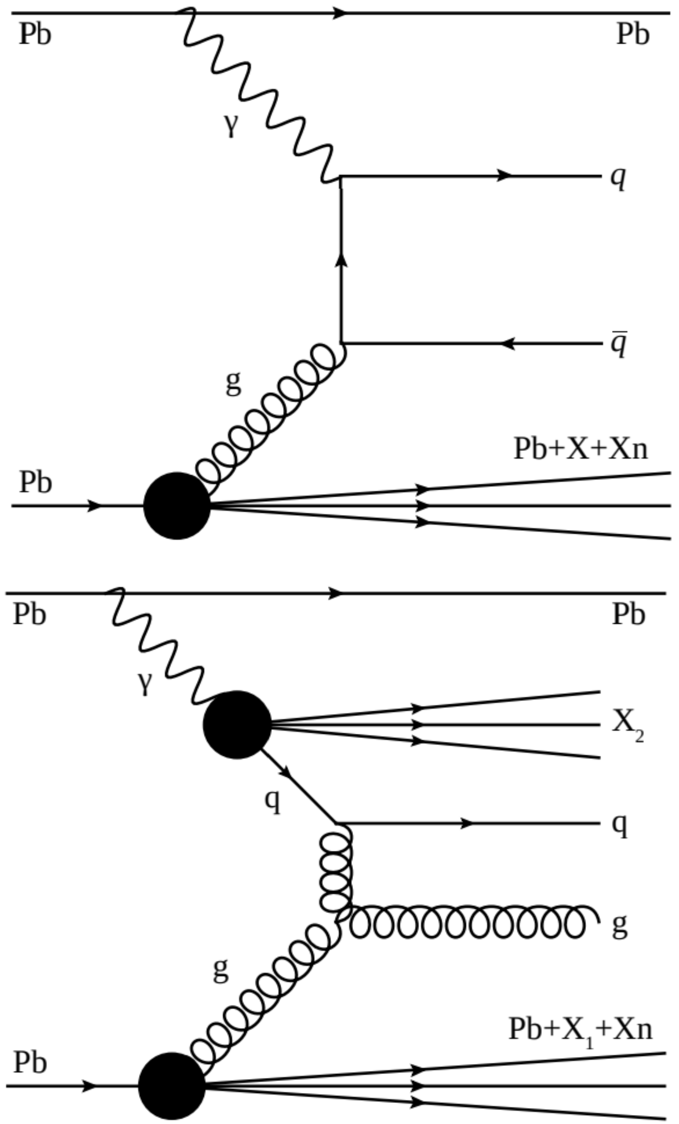

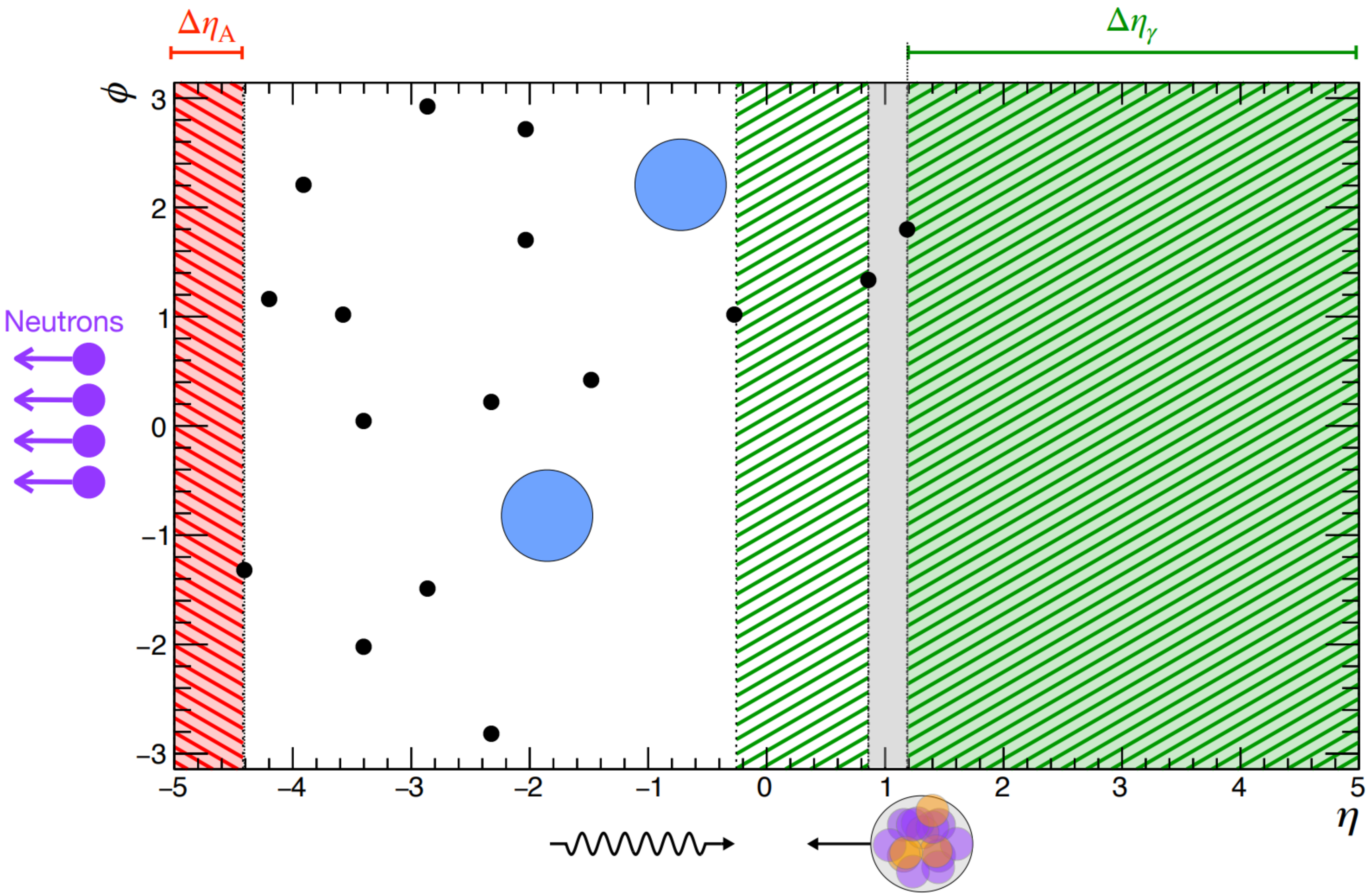

Photonuclear Jet Production

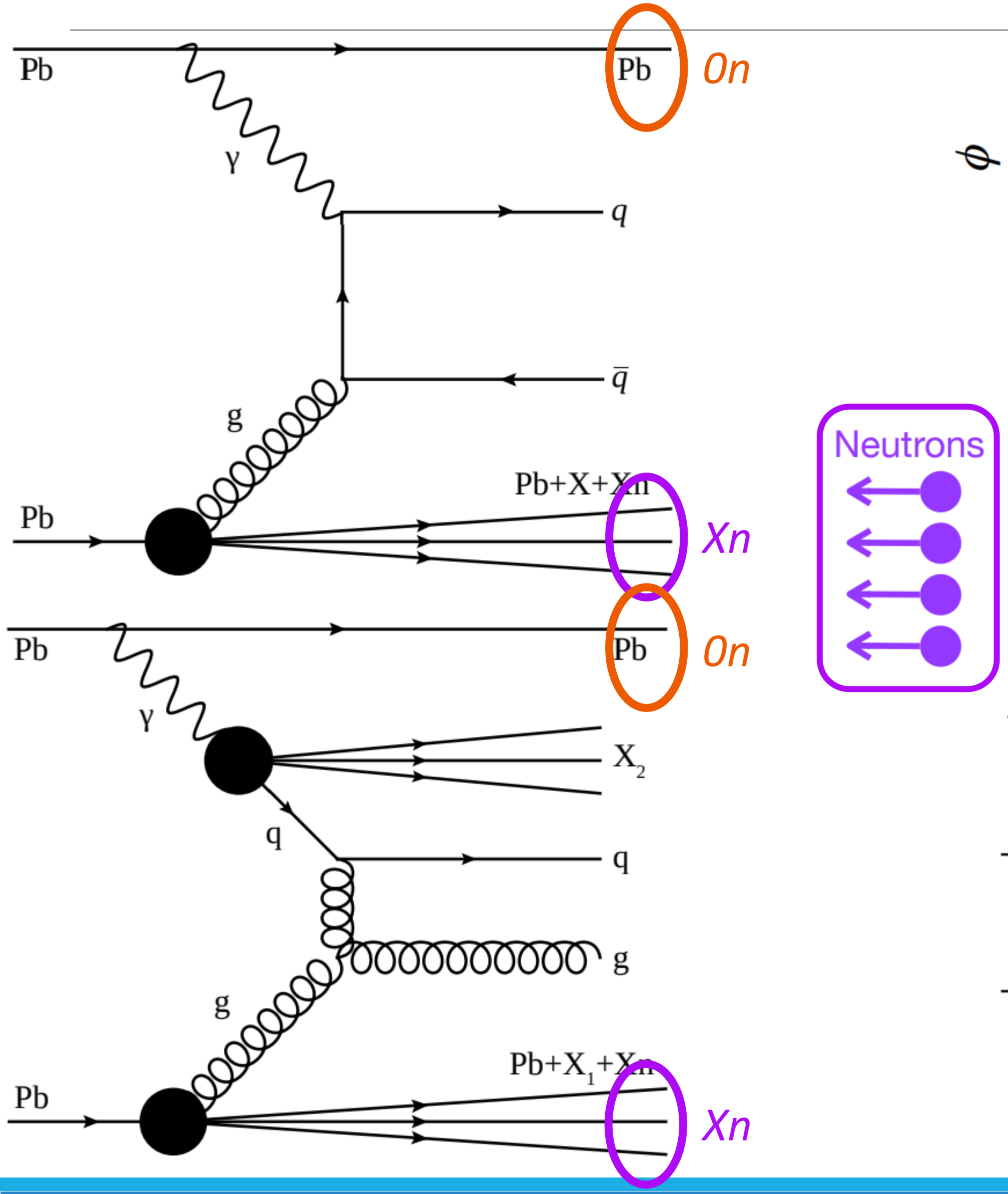

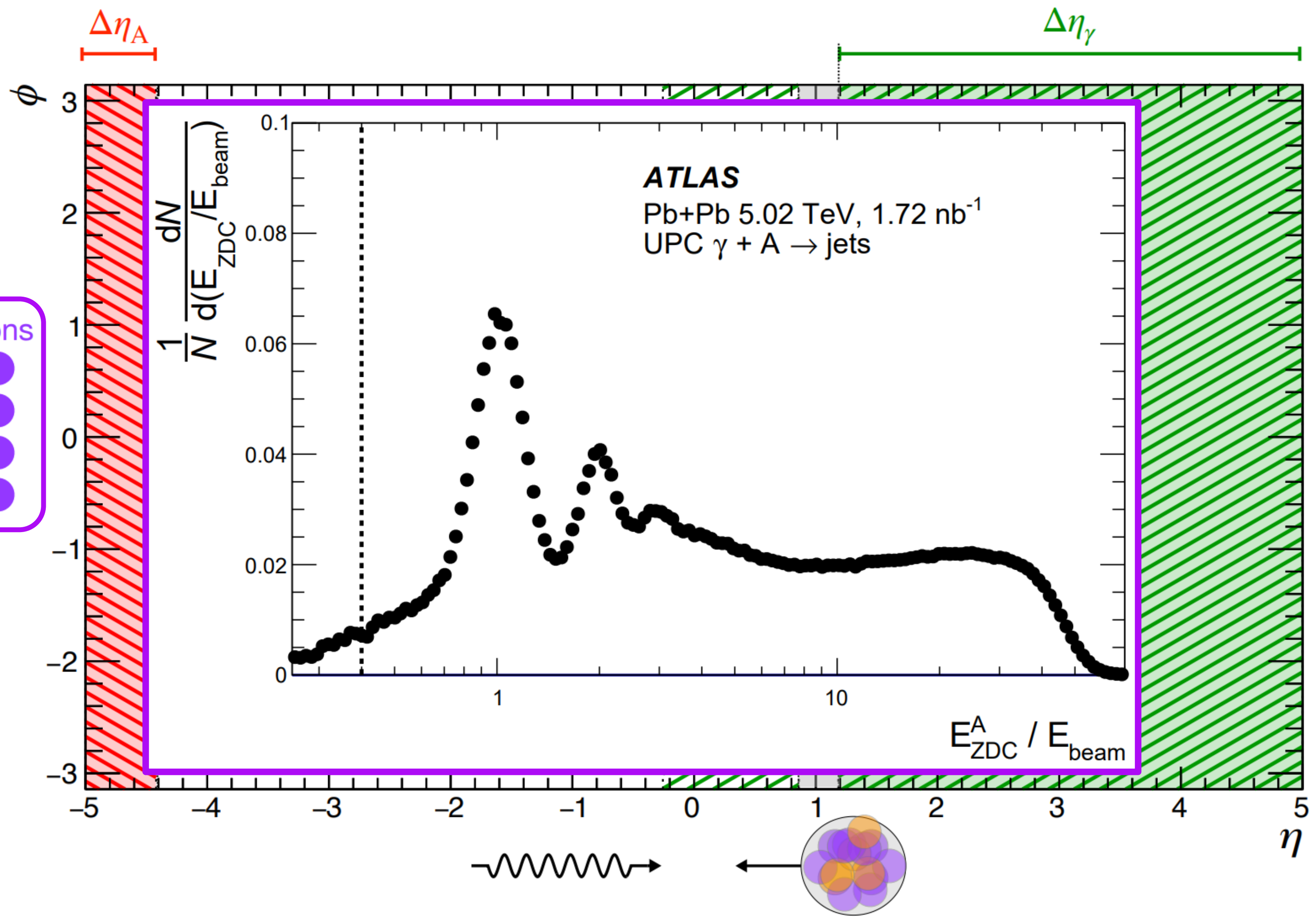

Photonuclear Jet Production

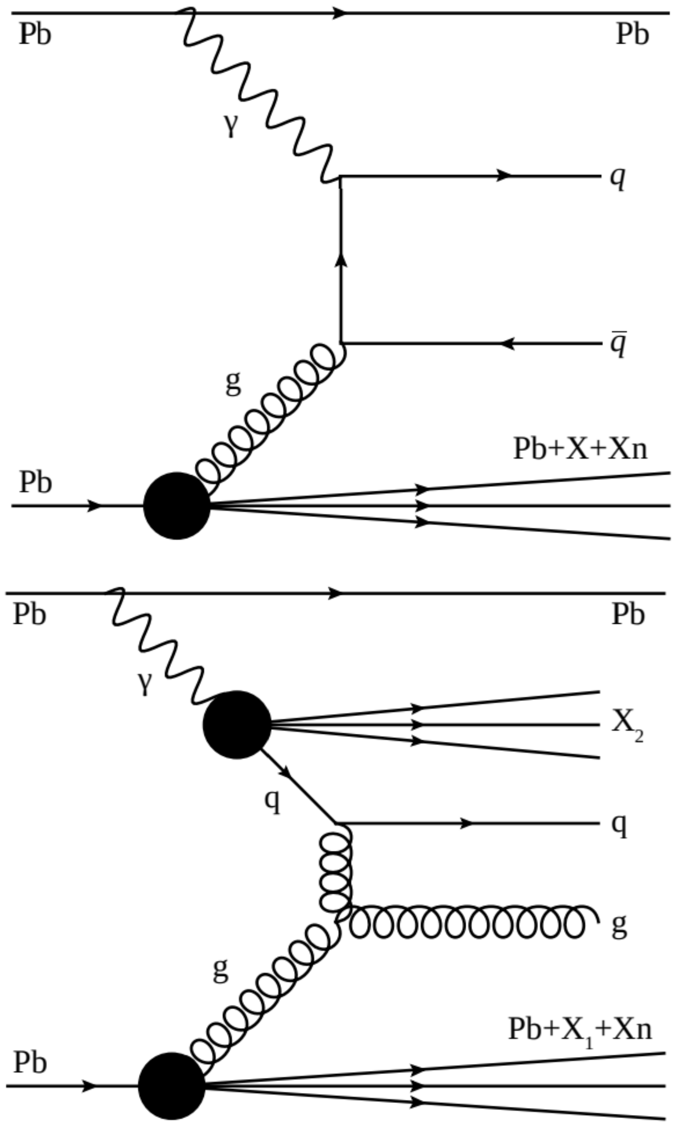

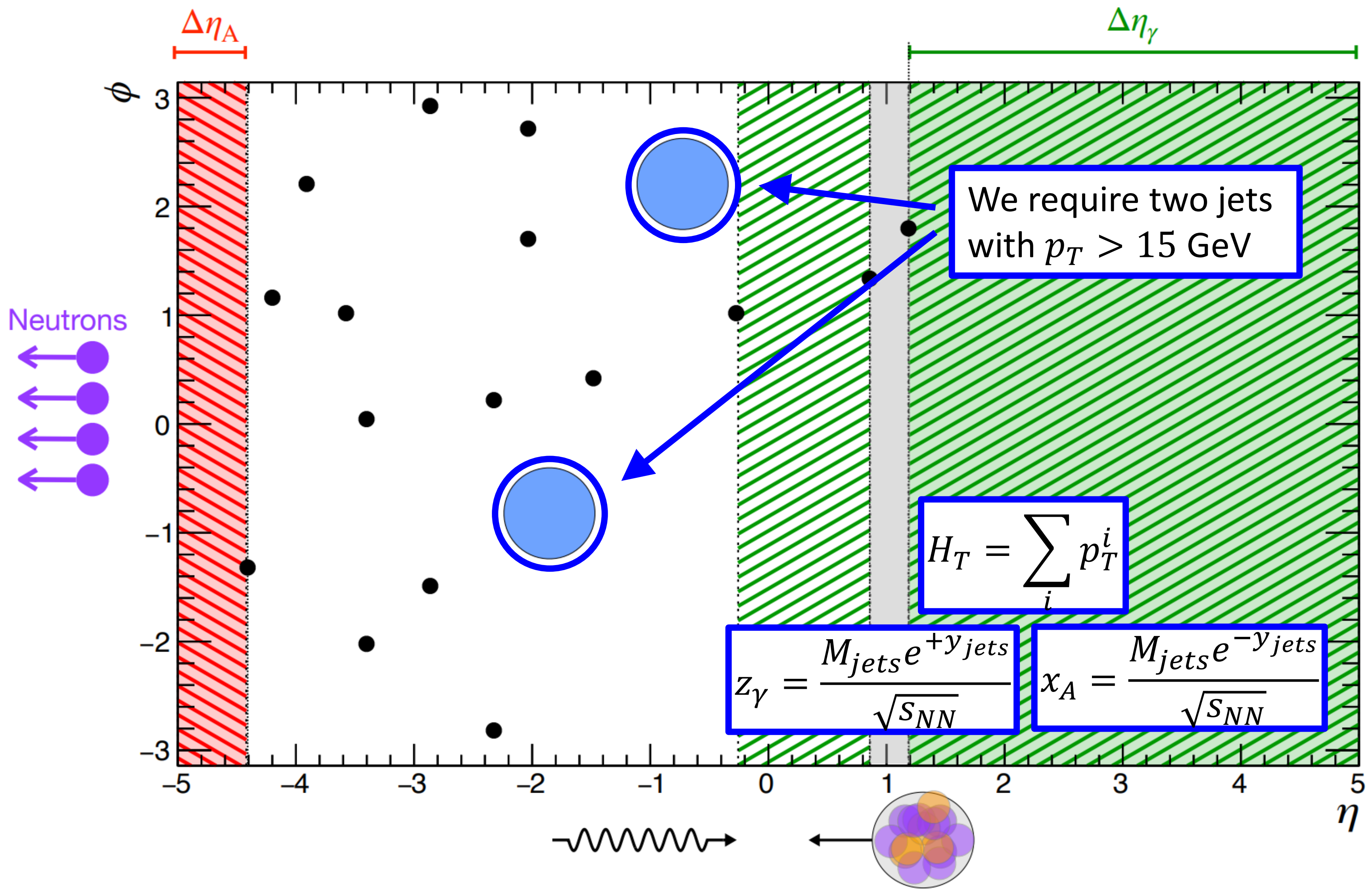

Photonuclear Jet Production

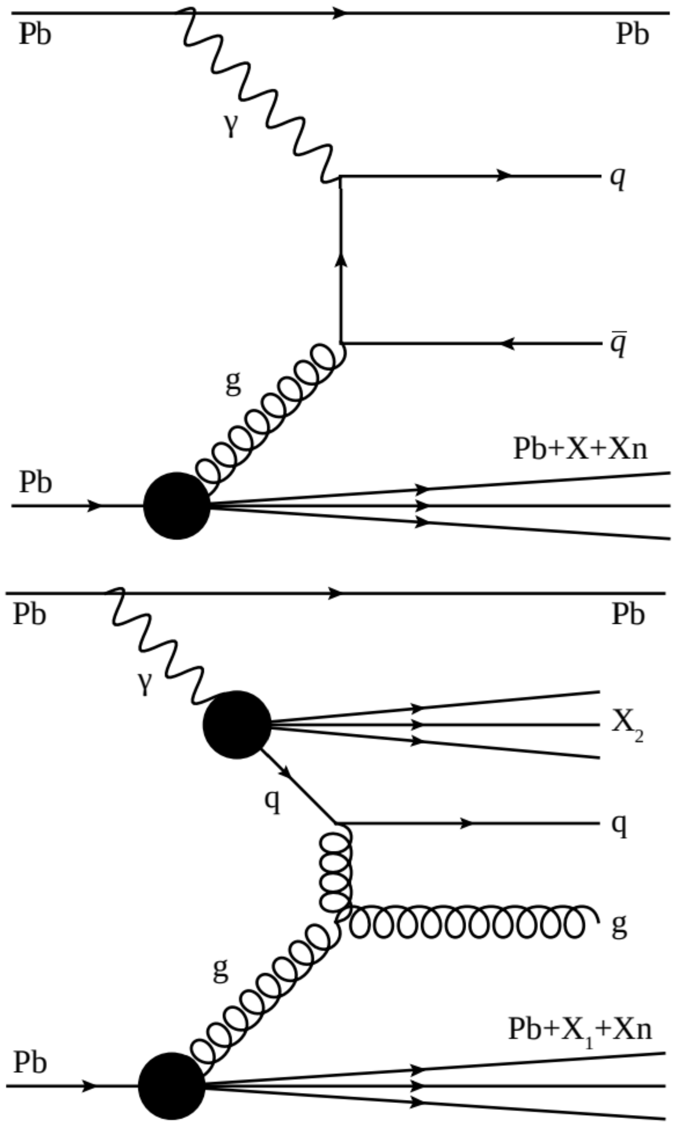

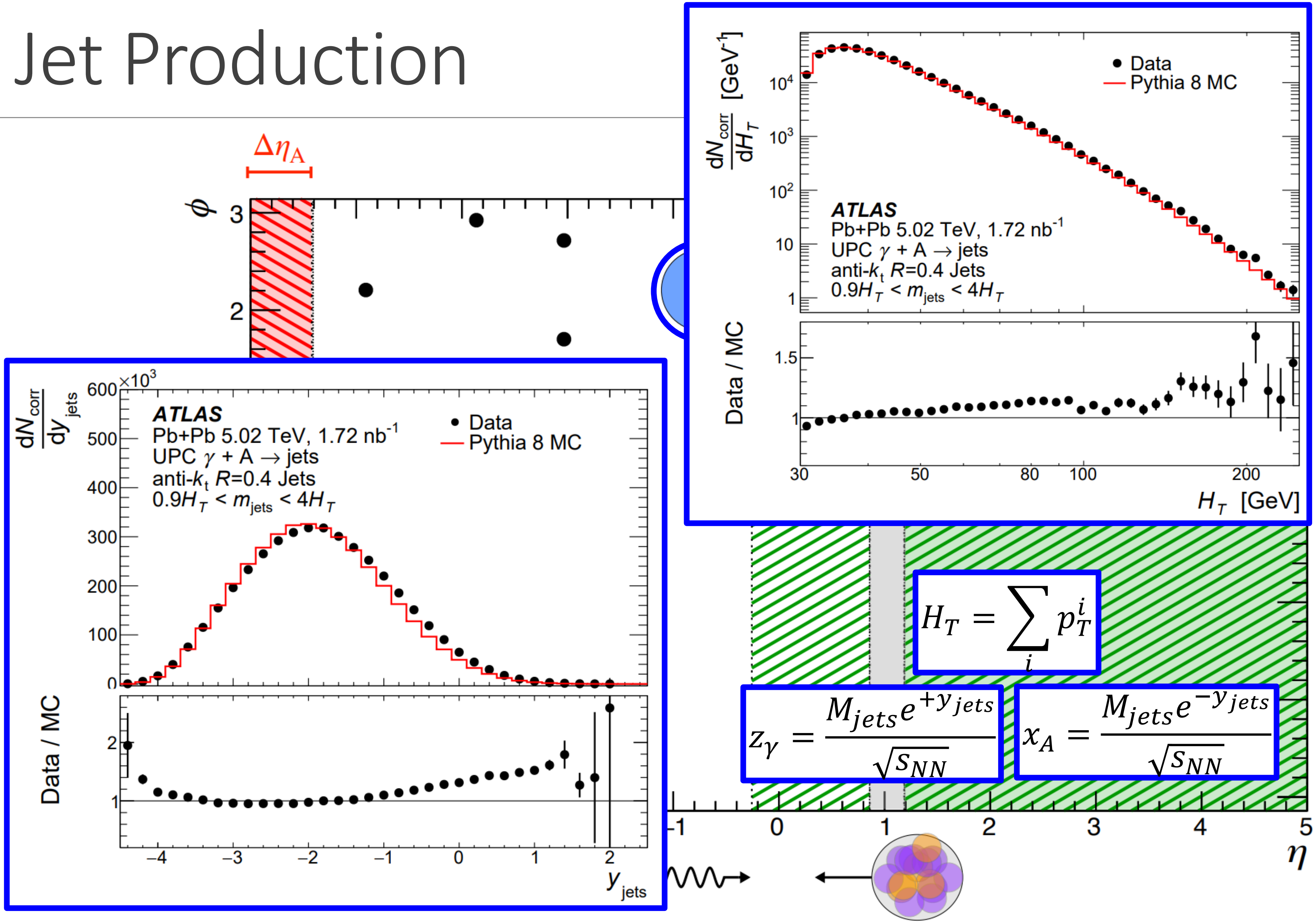

$$H_T = \sum_i p_T^i$$

$$z_\gamma = \frac{M_{jets} e^{+y_{jets}}}{\sqrt{s_{NN}}}$$

$$x_A = \frac{M_{jets} e^{-y_{jets}}}{\sqrt{s_{NN}}}$$

Photonuclear Jet Production

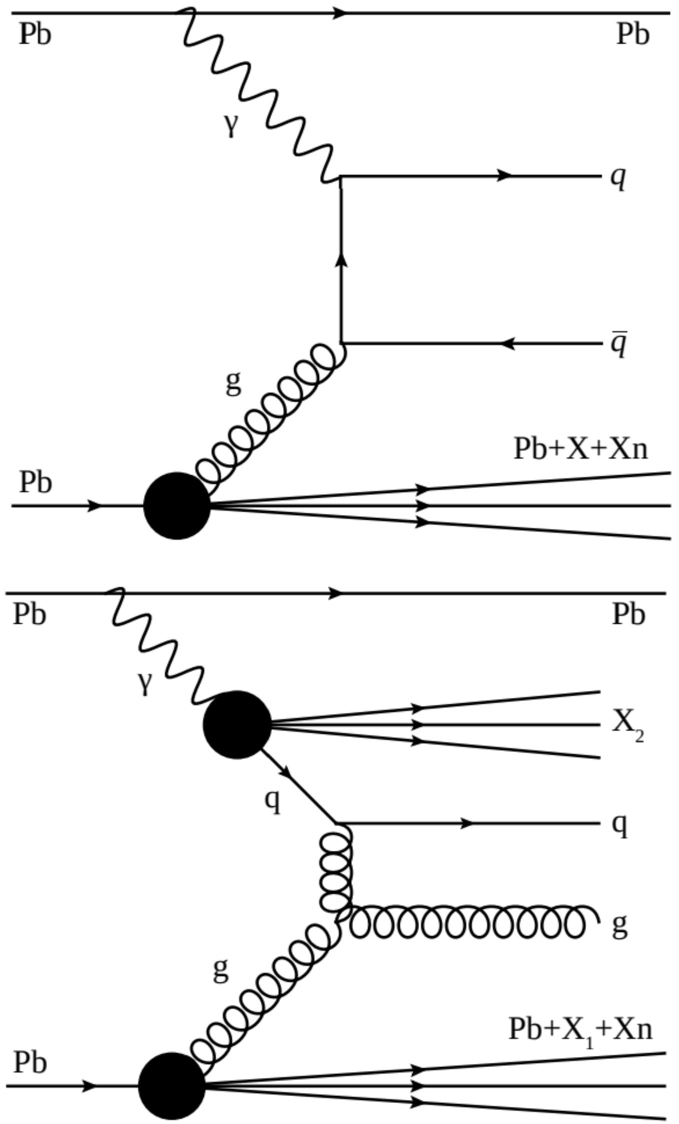

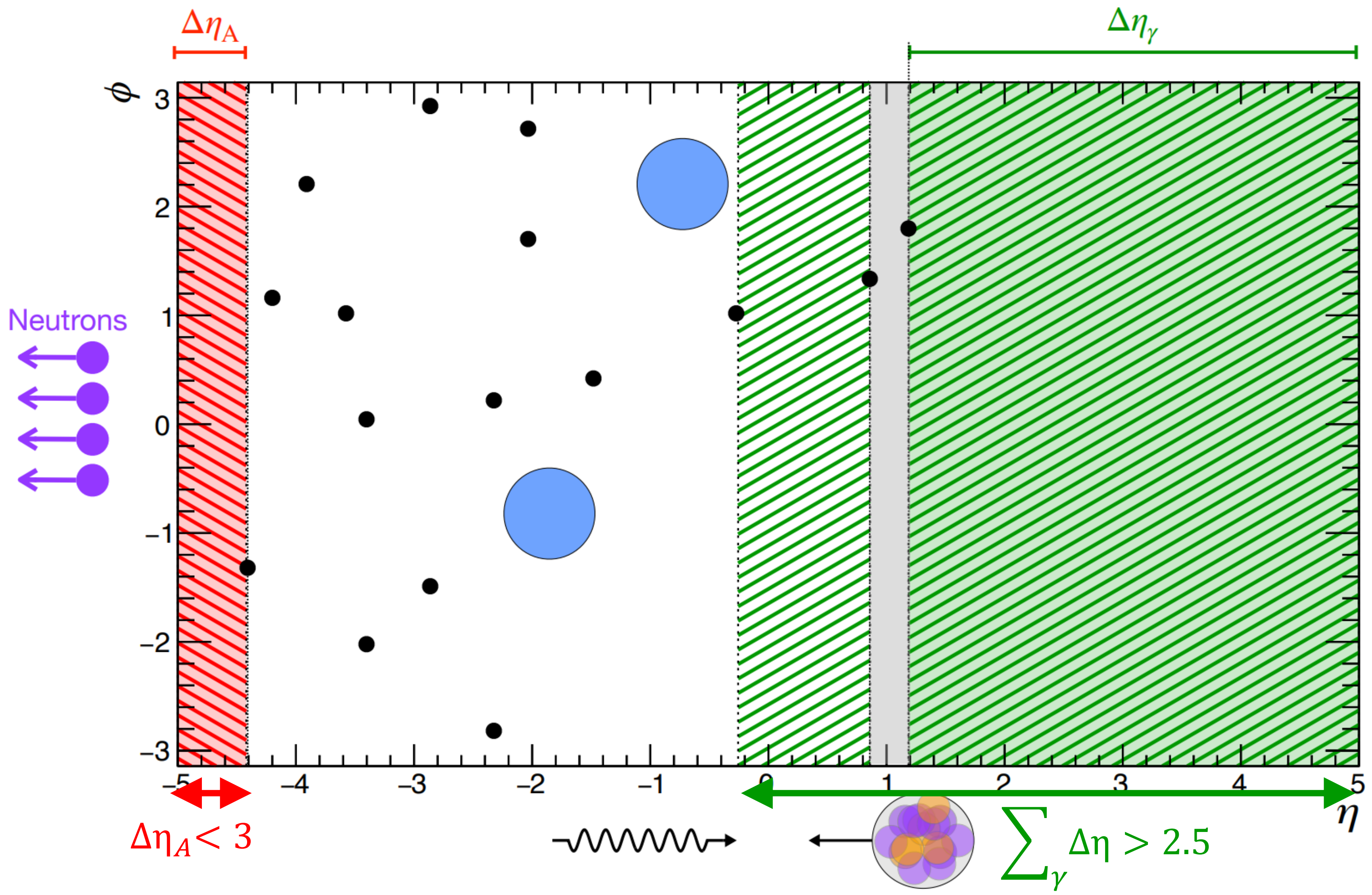

Photonuclear Jet Production

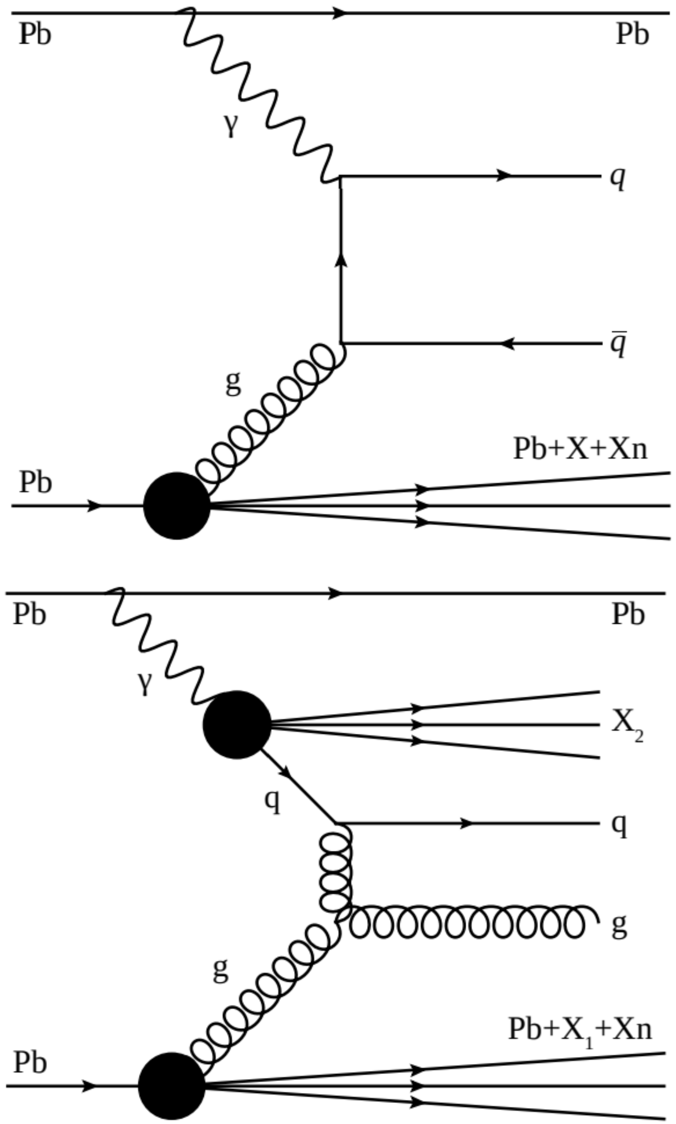

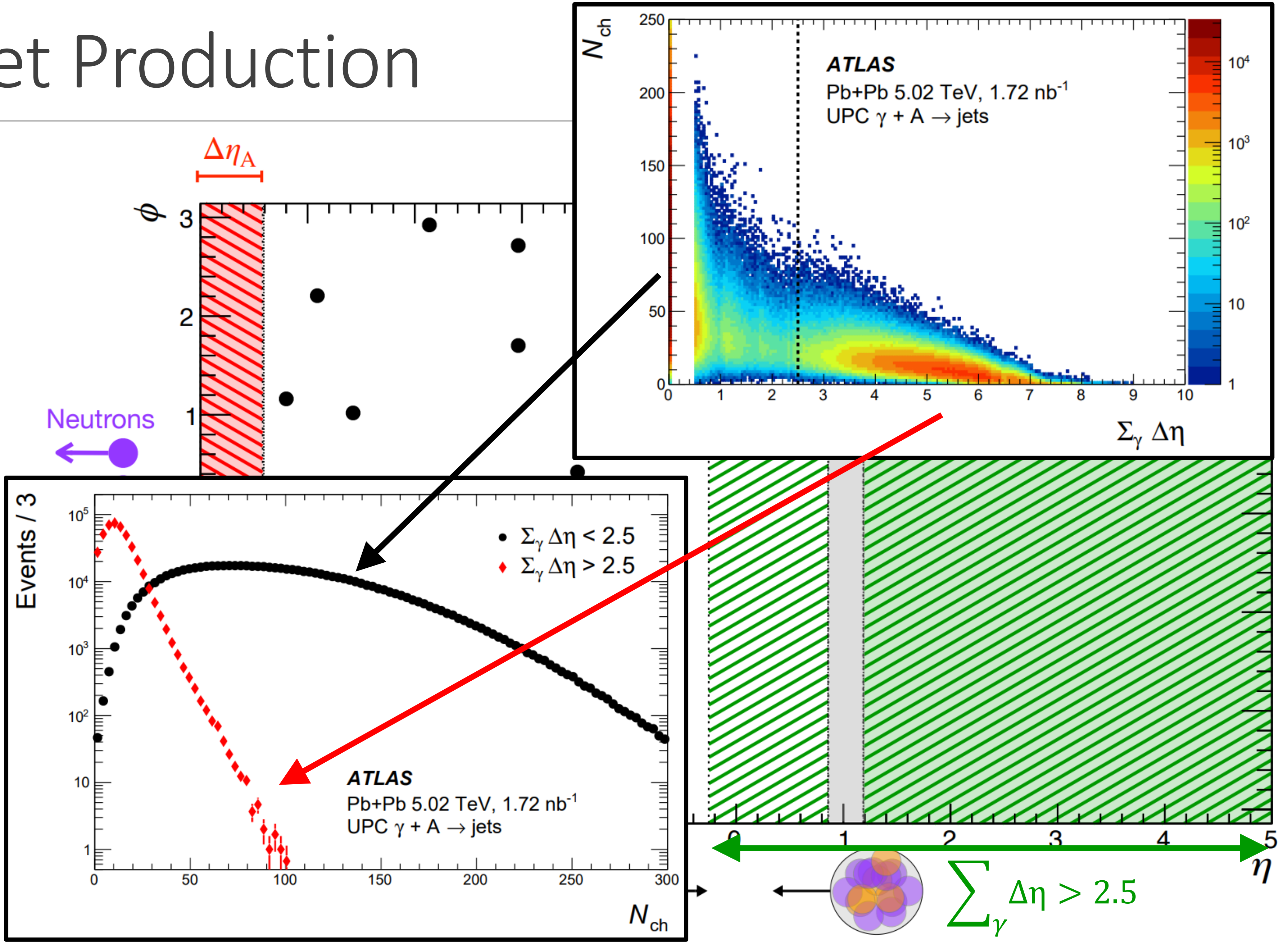

Gap Selections and Photon Structure

$$z_\gamma = \frac{M_{jets} e^{+y_{jets}}}{\sqrt{s_{NN}}}$$

- Template fit studies of $\sum_\gamma \Delta\eta$ provide two pieces of information:
  - The efficacy and background contamination rates for different gap selections
  - The relative proportion of direct and resolved photon events

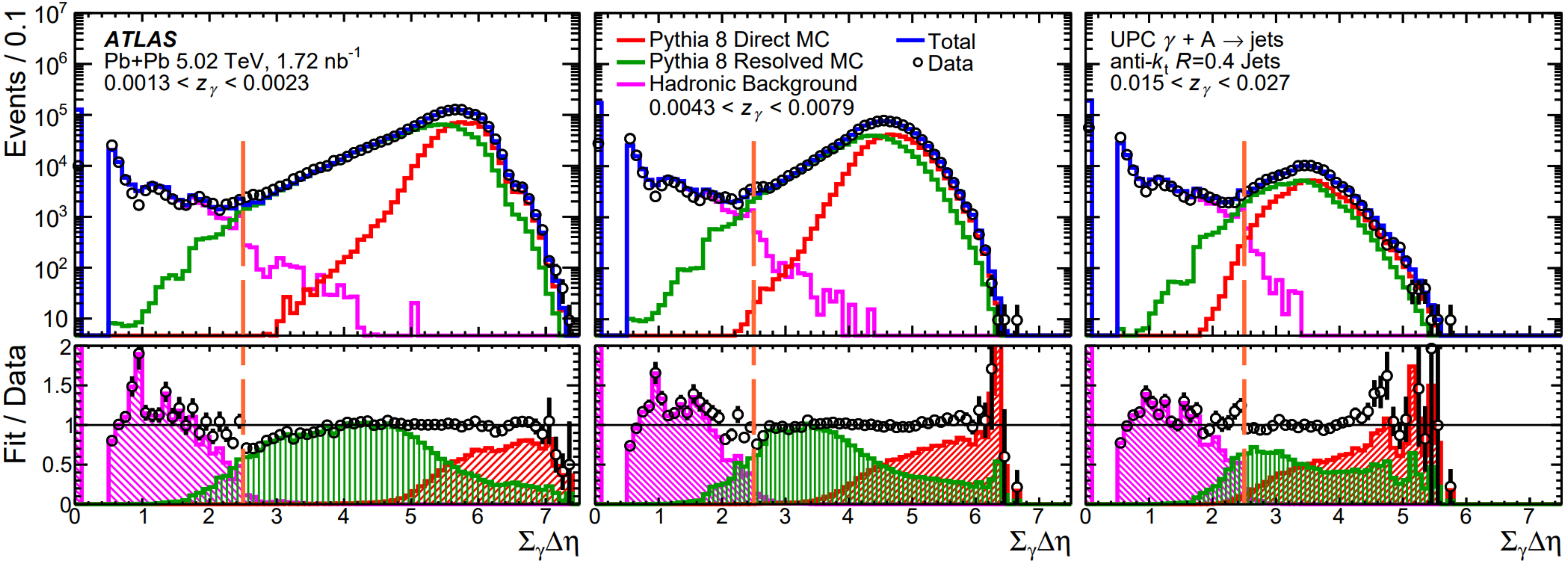

Gap Selections and Photon Structure

$$H_T = \sum_i p_T^i$$

$$z_\gamma = \frac{M_{jets} e^{+y_{jets}}}{\sqrt{s_{NN}}}$$

- The selection we apply (red) retains a sufficient level of signal purity.

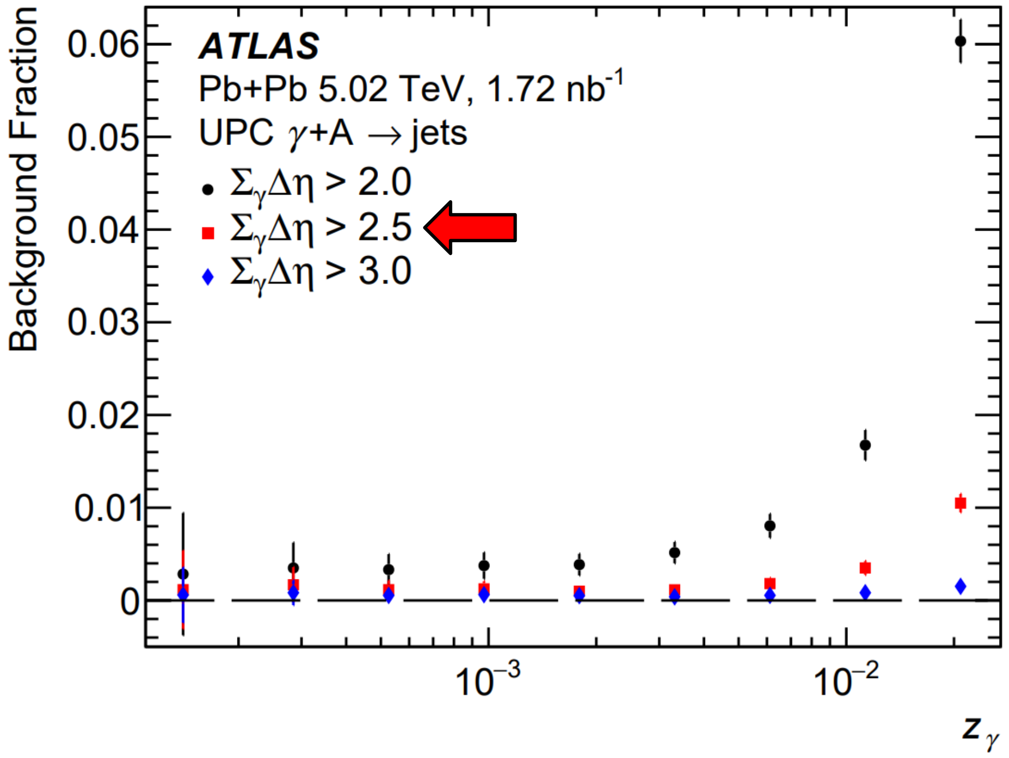

Gap Selections and Photon Structure

$$H_T = \sum_i p_T^i$$

$$z_\gamma = \frac{M_{jets} e^{+y_{jets}}}{\sqrt{s_{NN}}}$$

- The selection we apply (red) retains a sufficient level of signal purity.
- The direct fraction differs between data and theory at low H_T but is well-modeled at high H_T.

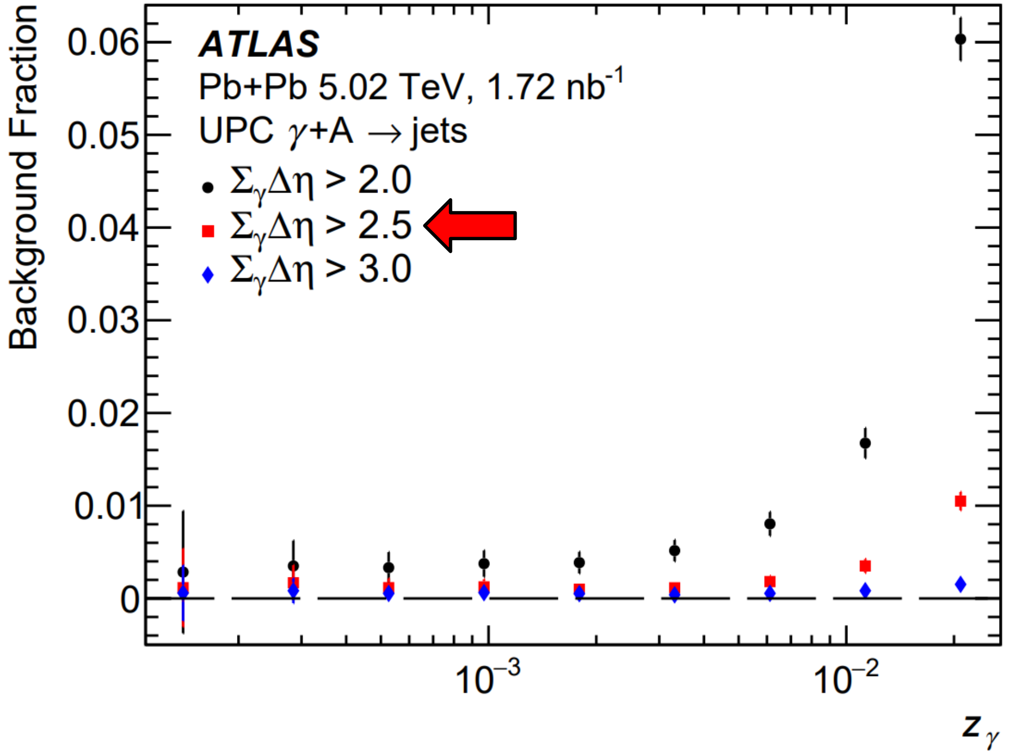

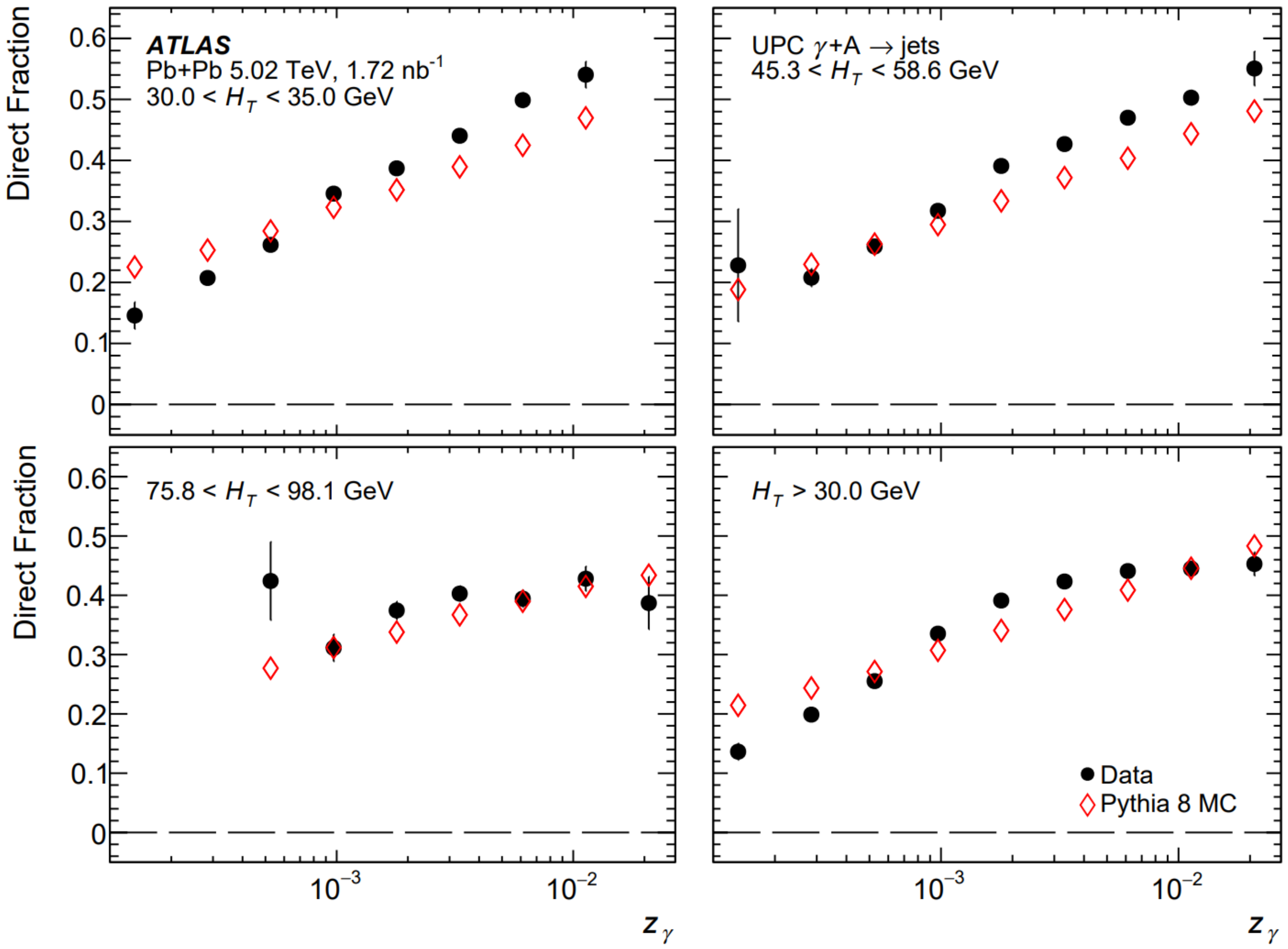

Measuring Nuclear Breakup

The photonuclear jet requirements select events with very high-energy photons.

- $E_\gamma \propto 1/b \rightarrow$ Biases towards lower impact parameter collisions
- Much higher probability of breakup of the photon-emitting nucleus due to additional EM interactions

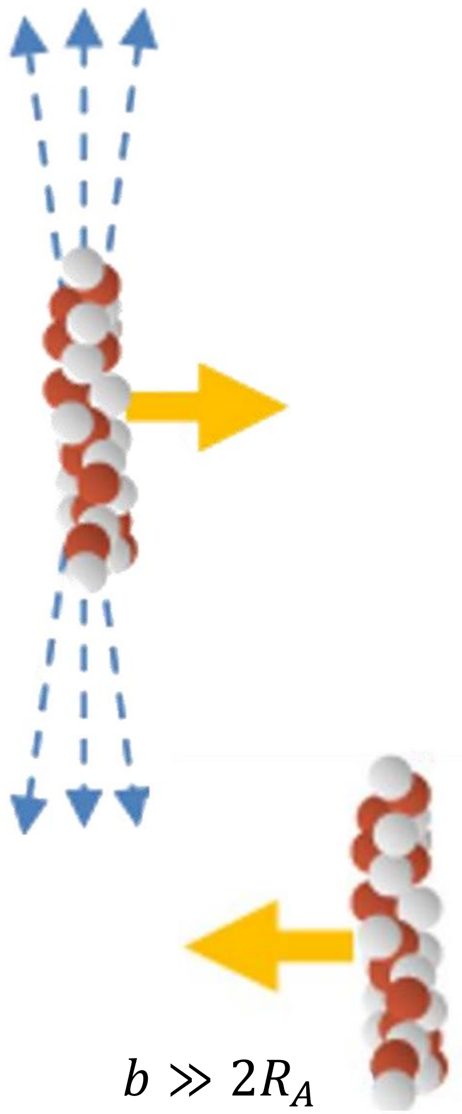

$b \gg 2R_A$

Measuring Nuclear Breakup

The photonuclear jet requirements select events with very high-energy photons.

- $E_\gamma \propto 1/b \rightarrow$ Biases towards lower impact parameter collisions
- Much higher probability of breakup of the photon-emitting nucleus due to additional EM interactions

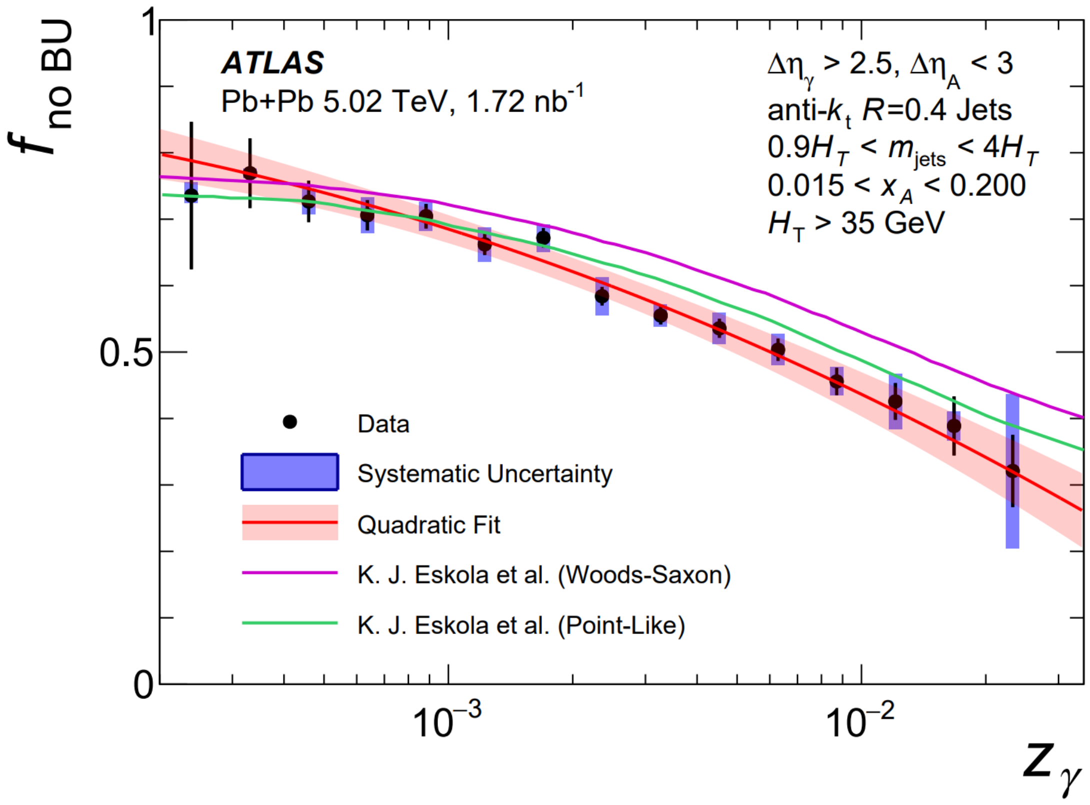

$$f_{\text{no BU}} \equiv \frac{d\sigma/dz_\gamma|_{0nXn}}{d\sigma/dz_\gamma|_{XnXn} + d\sigma/dz_\gamma|_{0nXn}}$$

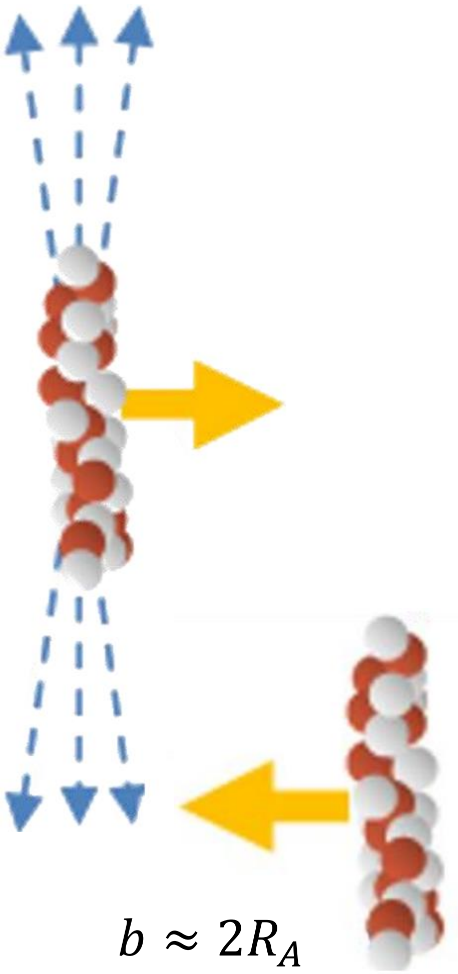

$b \approx 2R_A$

Measuring Nuclear Breakup

The photonuclear jet requirements select events with very high-energy photons.

- $E_\gamma \propto 1/b \rightarrow$ Biases towards lower impact parameter collisions
- Much higher probability of breakup of the photon-emitting nucleus due to additional EM interactions

This measured correction for breakup is used to compare theory to data.

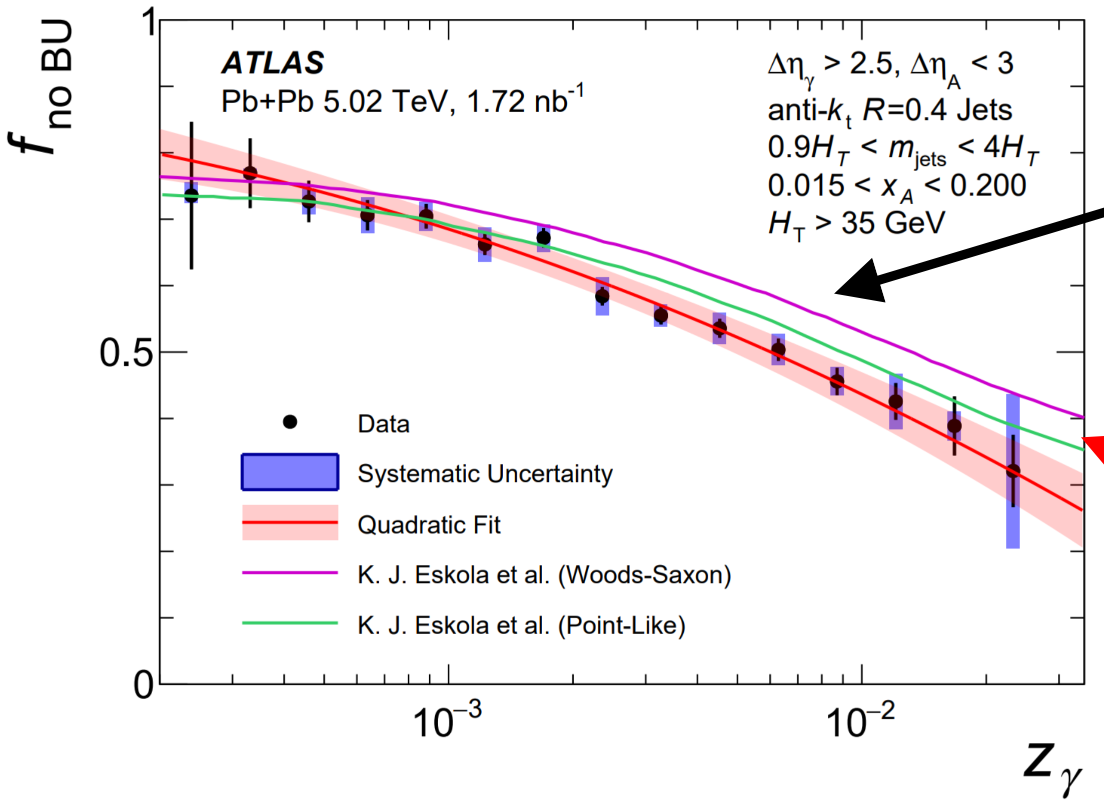

$$f_{\text{no BU}} \equiv \frac{d\sigma/dz_\gamma|_{0nXn}}{d\sigma/dz_\gamma|_{XnXn} + d\sigma/dz_\gamma|_{0nXn}}$$

Measurements of the breakup rate in XnXn and 0nXn events show that about 50% of photo-nuclear jet production breaks up!

Theoretical modeling predicts the rate well but misses slightly at large z_γ. (arXiv:2404.09731)

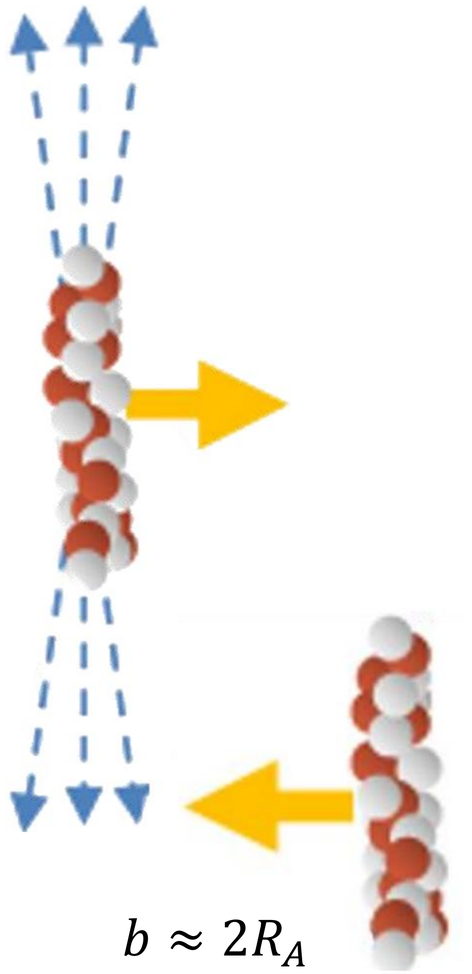

$b \approx 2R_A$

Systematic Uncertainties

Systematic uncertainties are the key limiting factor in our sensitivity to nuclear PDFs.

The jet energy scale and resolution uncertainties are typically 5-10%. These uncertainties are highly correlated between bins.

Systematic uncertainties are also evaluated on the unfolding and event selections. These uncertainties are treated as un-correlated.

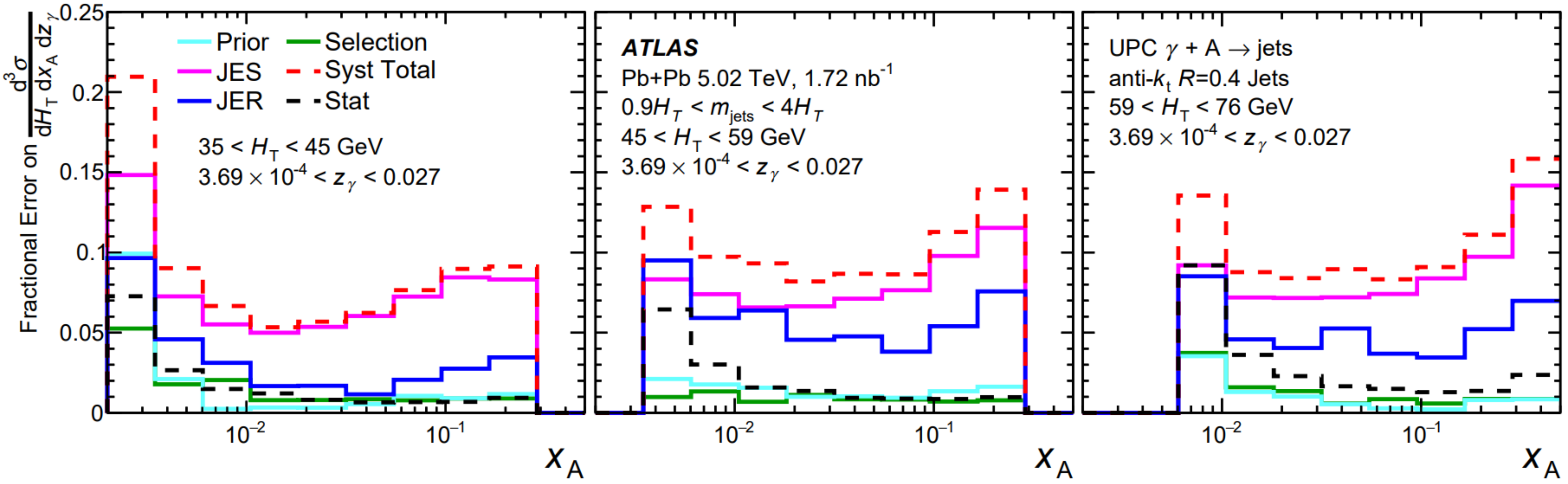

UPC Dijets: Scanning in Photon Energy

$$H_T = \sum_i p_T^i \qquad x_A = \frac{M_{jets} e^{-y_{jets}}}{\sqrt{s_{NN}}} \qquad z_\gamma = \frac{M_{jets} e^{+y_{jets}}}{\sqrt{s_{NN}}}$$

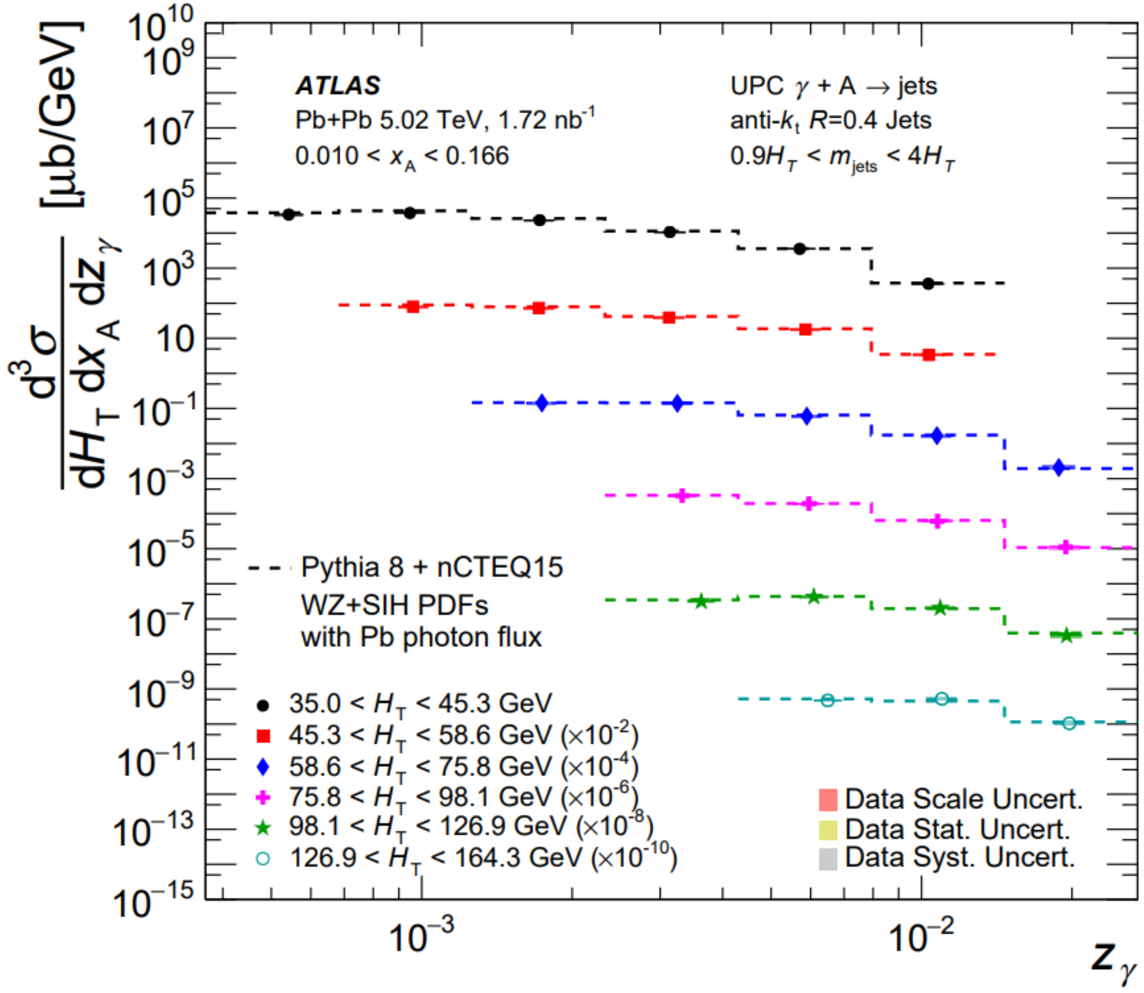

The x_A distribution has substantial acceptance effects in z_γ.

Selecting on photon energy removes this bias, allowing a more direct measurement of nPDFs.

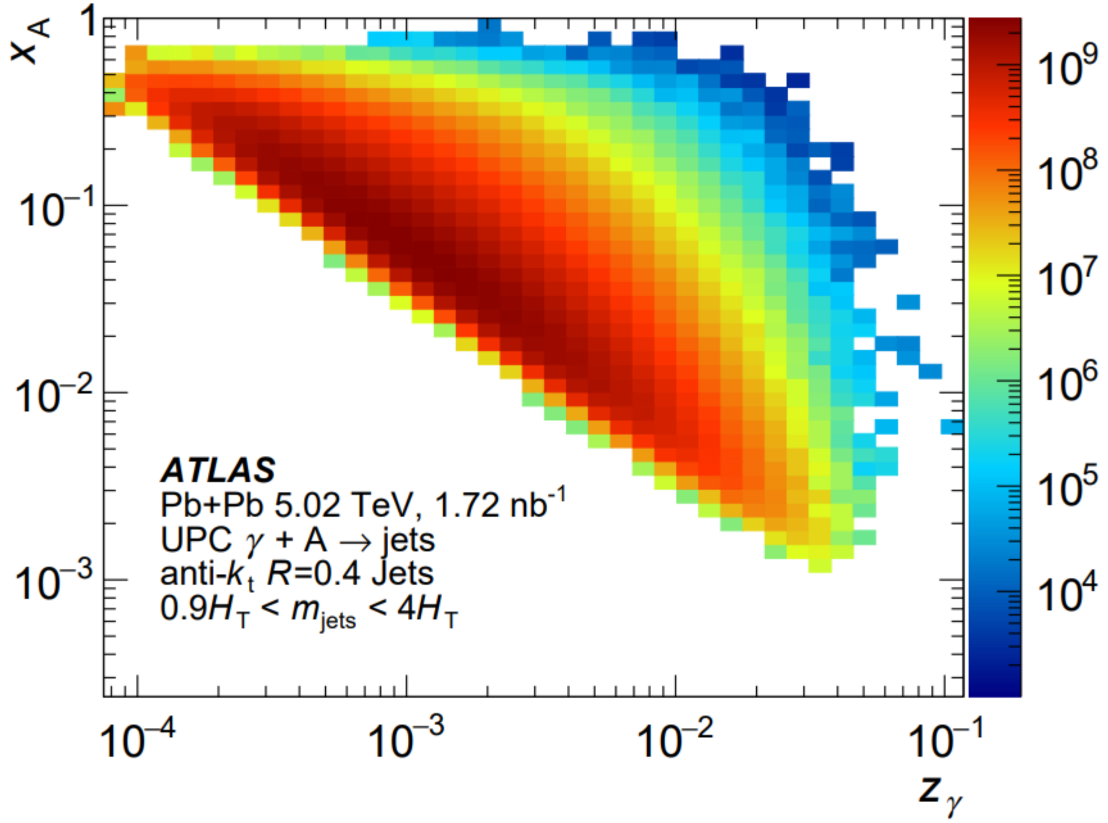

UPC Dijets: Scanning in Photon Energy

$$H_T = \sum_i p_T^i \qquad x_A = \frac{M_{jets} e^{-y_{jets}}}{\sqrt{s_{NN}}} \qquad z_\gamma = \frac{M_{jets} e^{+y_{jets}}}{\sqrt{s_{NN}}}$$

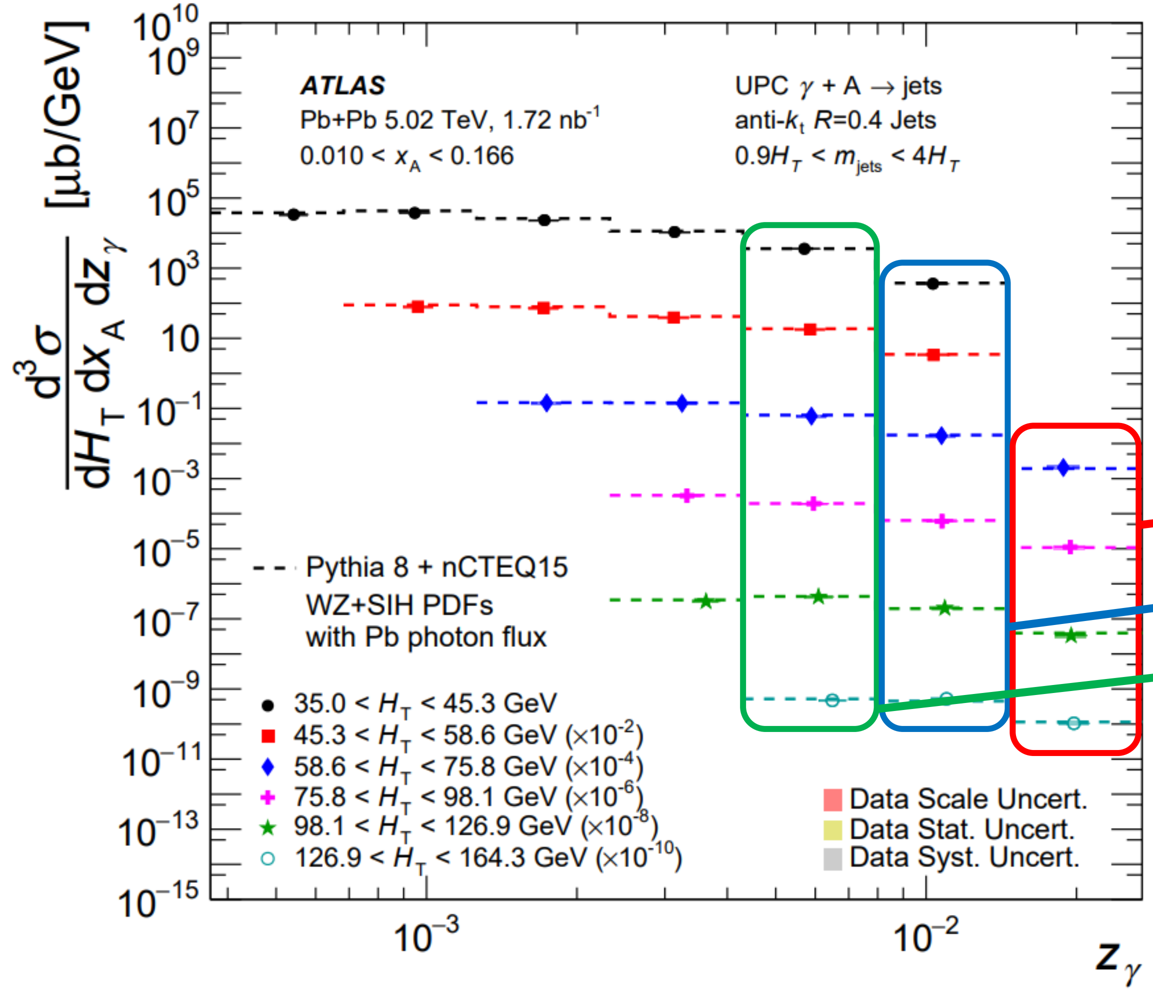

The x_A distribution has substantial acceptance effects in z_γ.

Selecting on photon energy removes this bias, allowing a more direct measurement of nPDFs.

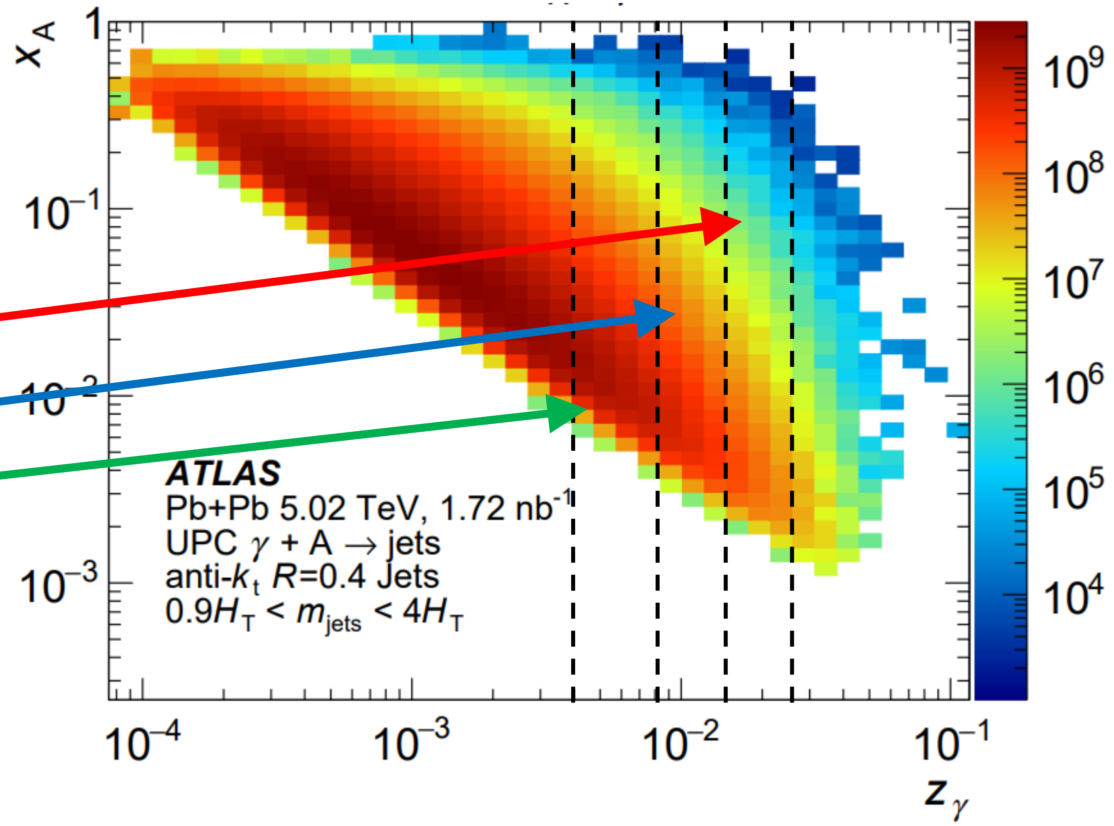

UPC Dijet Cross-Sections

- At lower photon energies, we can access higher-x partons.
- Systematic uncertainties are typically <5% in these bins after subtracting the correlated “scale” uncertainty.

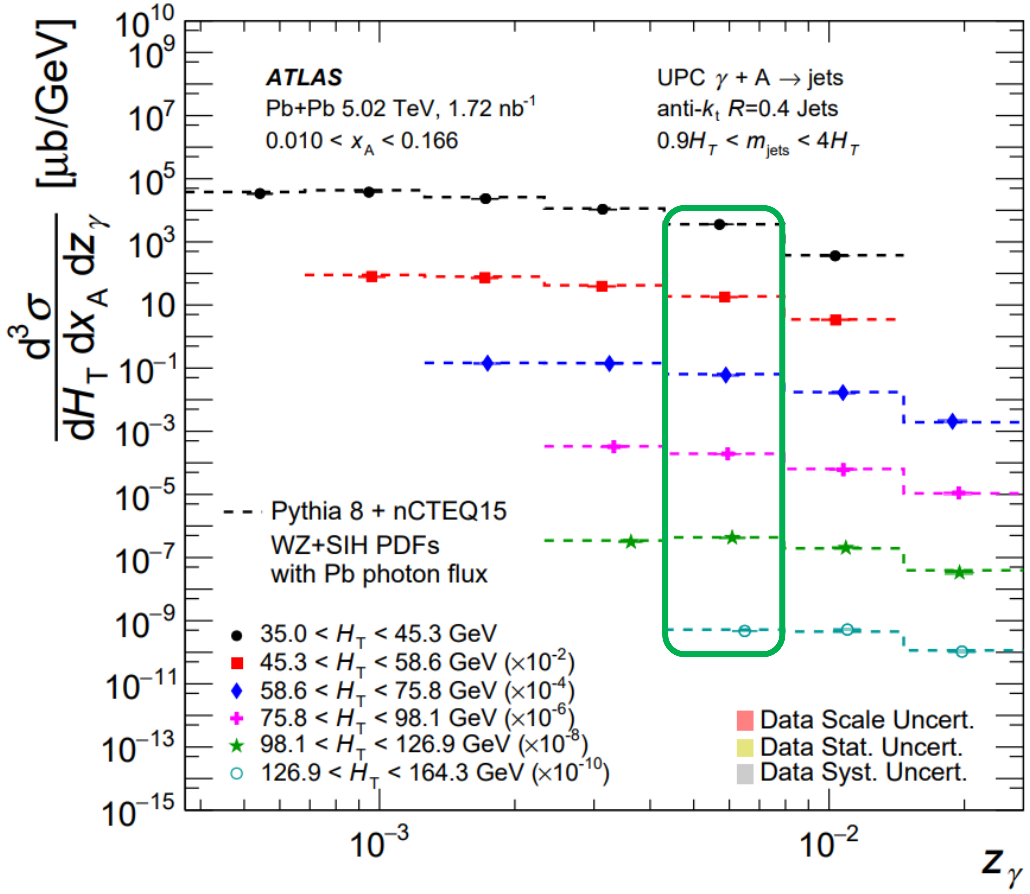

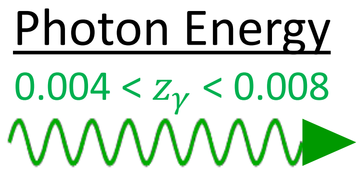

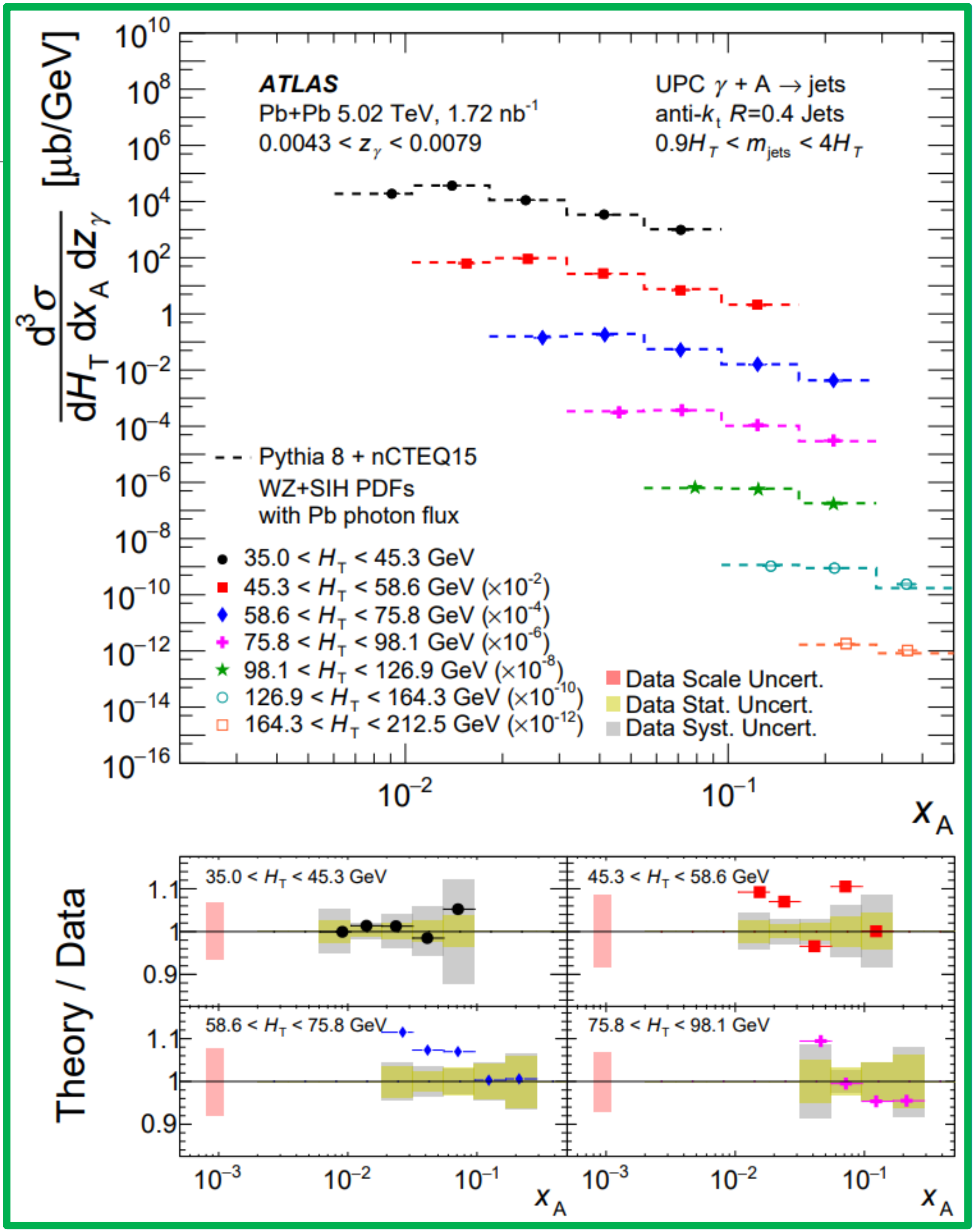

UPC Dijet Cross-Sections

- At intermediate photon energies, we begin to access the lower-x shadowing region.
- Systematic uncertainties are typically ~5% in these bins after subtracting the correlated “scale” uncertainty.

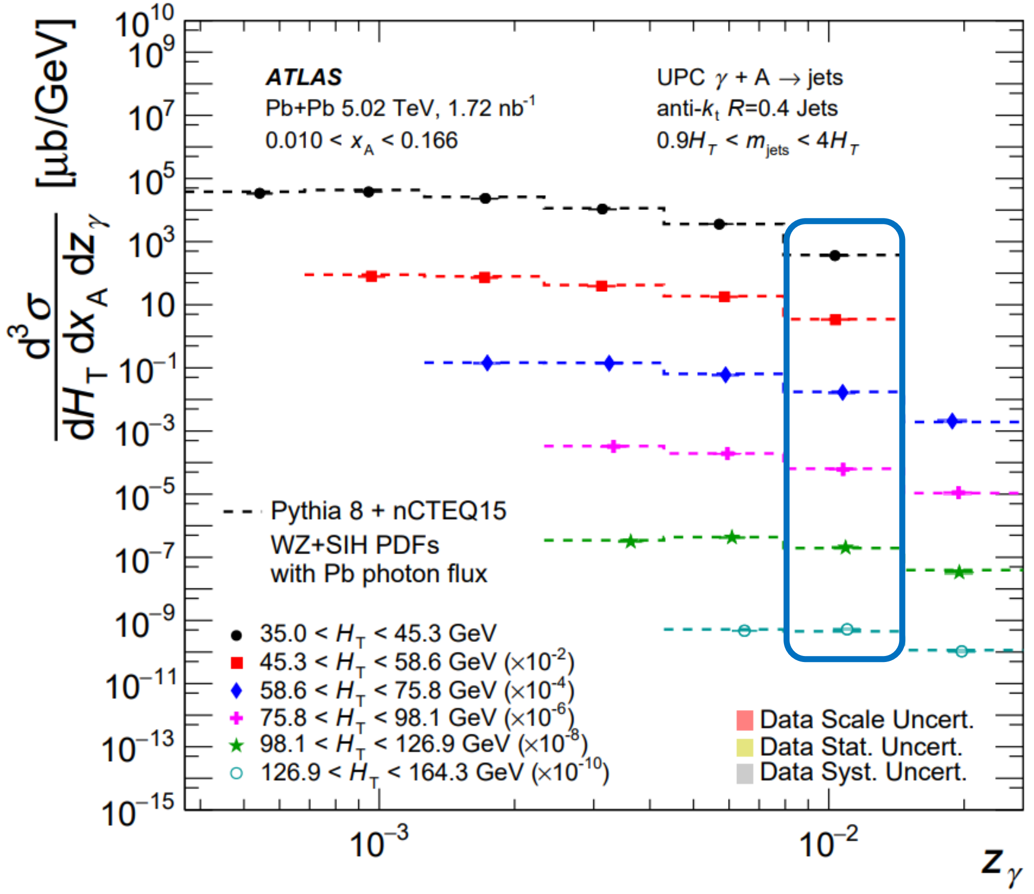

Photon Energy

$0.008 < z_\gamma < 0.015$

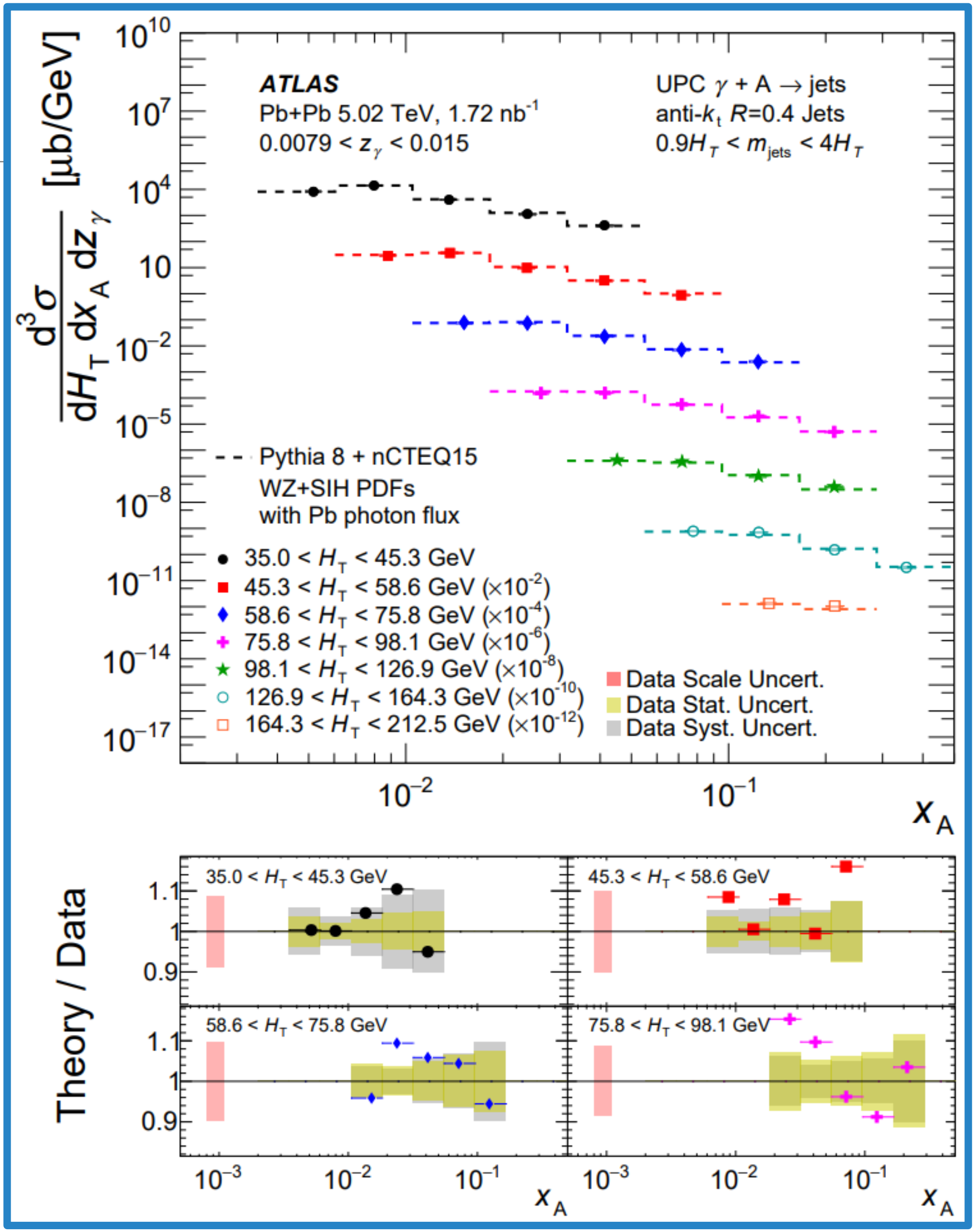

UPC Dijet Cross-Sections

- The highest photon energies allow access the shadowing region.
- Systematic uncertainties are typically ~5% in these bins after subtracting the correlated “scale” uncertainty.
  - The lowest-H_T bin is more challenging to constrain here.

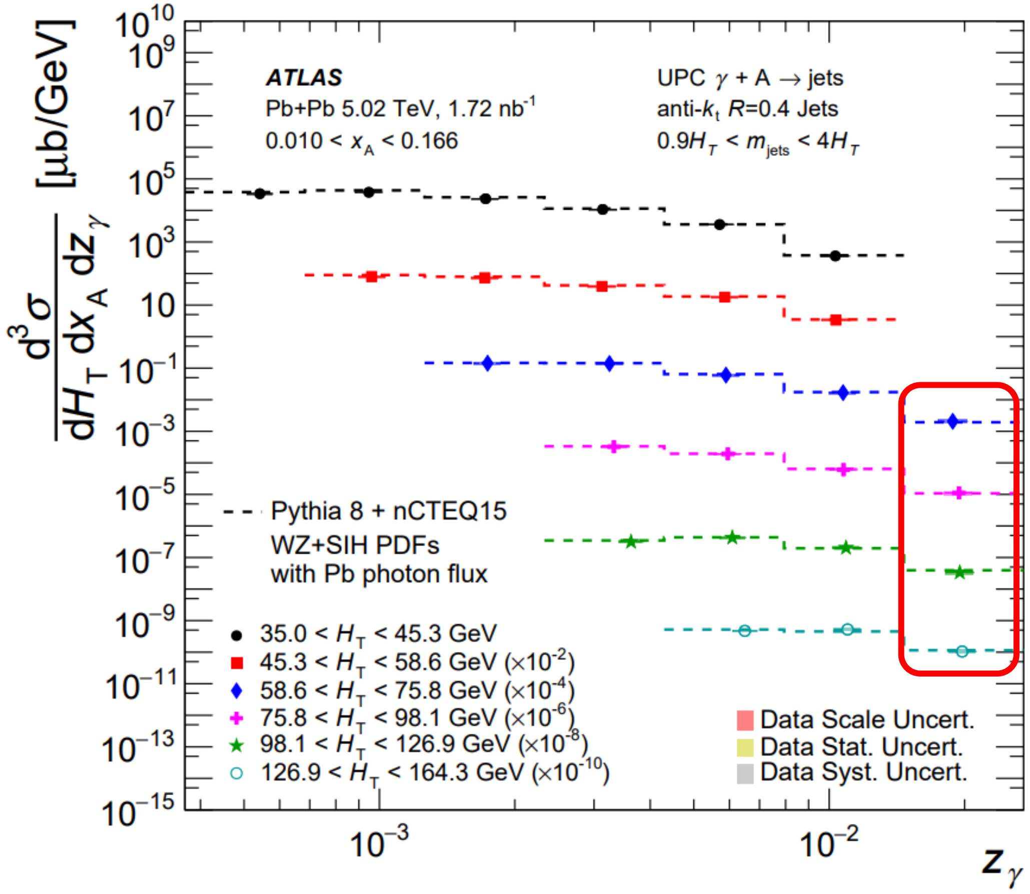

Photon Energy

$0.015 < z_\gamma < 0.027$

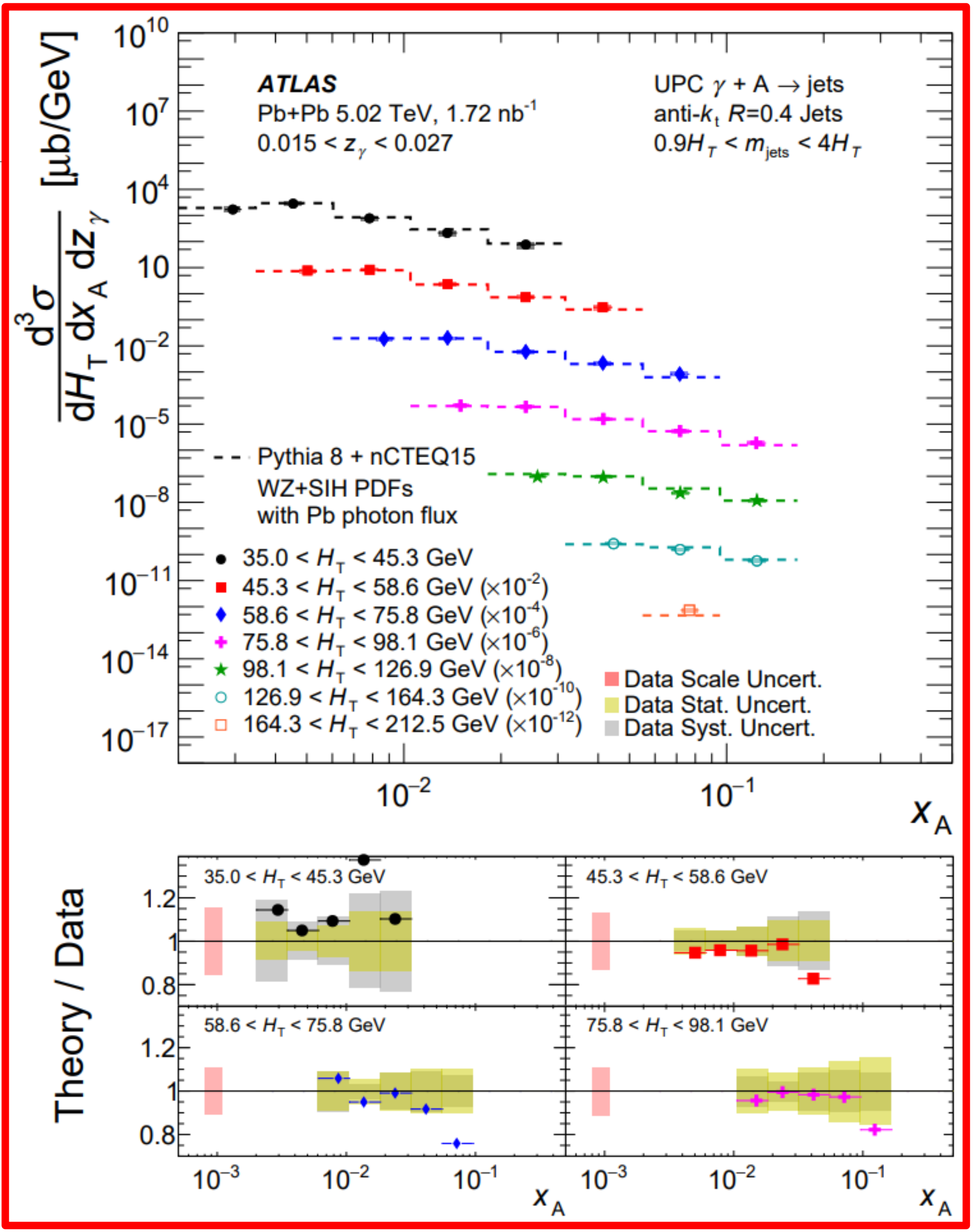

UPC Dijet Cross-Sections

- Integrating over photon energy provides the benefit of allowing the measurement over a broad range in x_A.
- In these bins, the uncertainty is typically ~5% after removing the scale uncertainty.

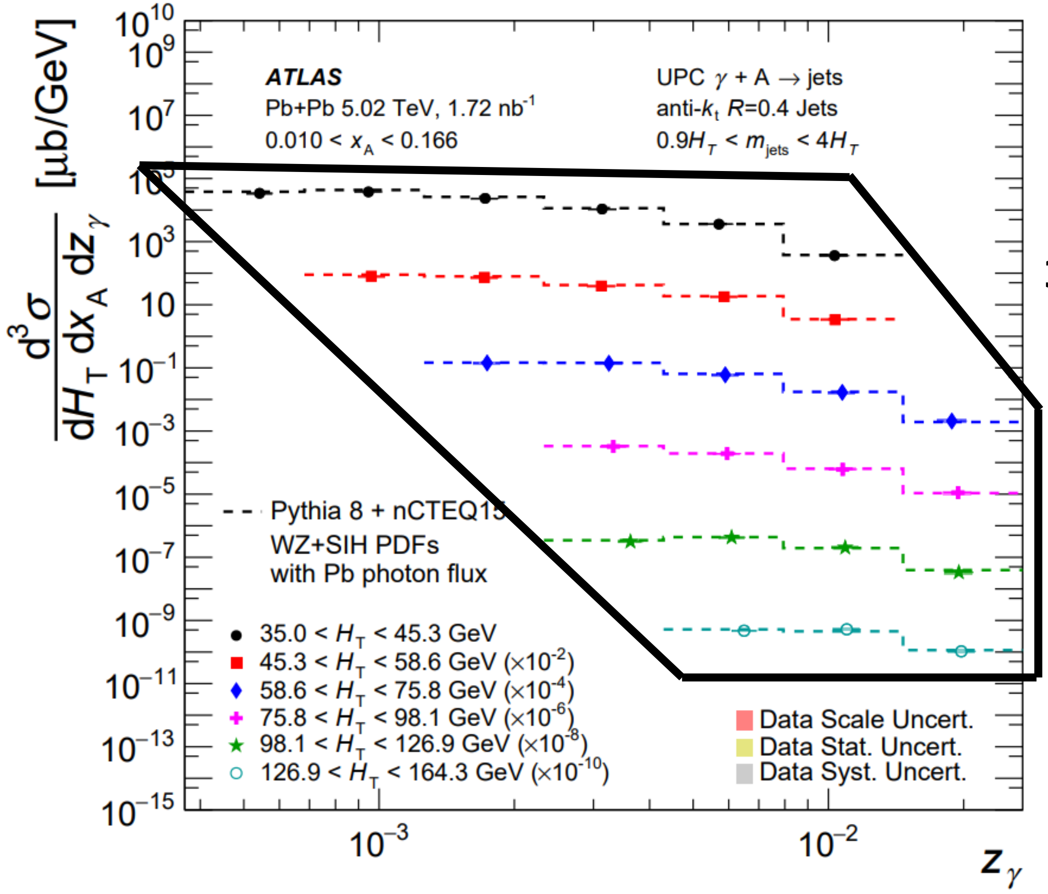

Photon Energy

$3.7 \times 10^{-4} < z_\gamma < 0.027$

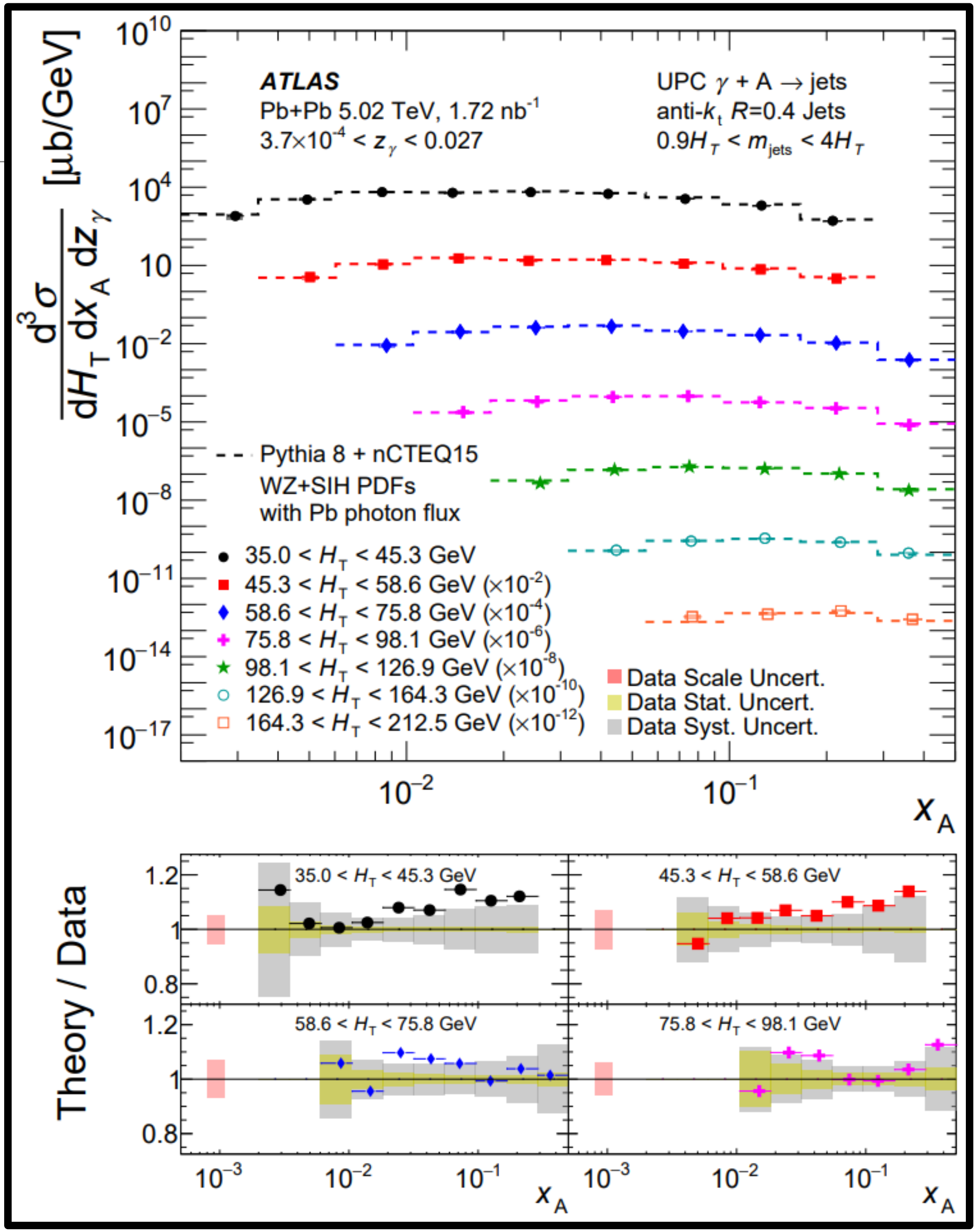

Comparing Across nPDFs

- This data can add a wide range of kinematic coverage to existing nPDF constraints.
  - All nPDF models have <u>excess anti-shadowing</u>, while nCTEQ15 WZ+SIH and TUJU21 agree with the shadowing observed in data at low H_T.
  - The full data tables allow for a complete treatment of <u>correlated uncertainties</u>, which will constrain nPDF effects even further.

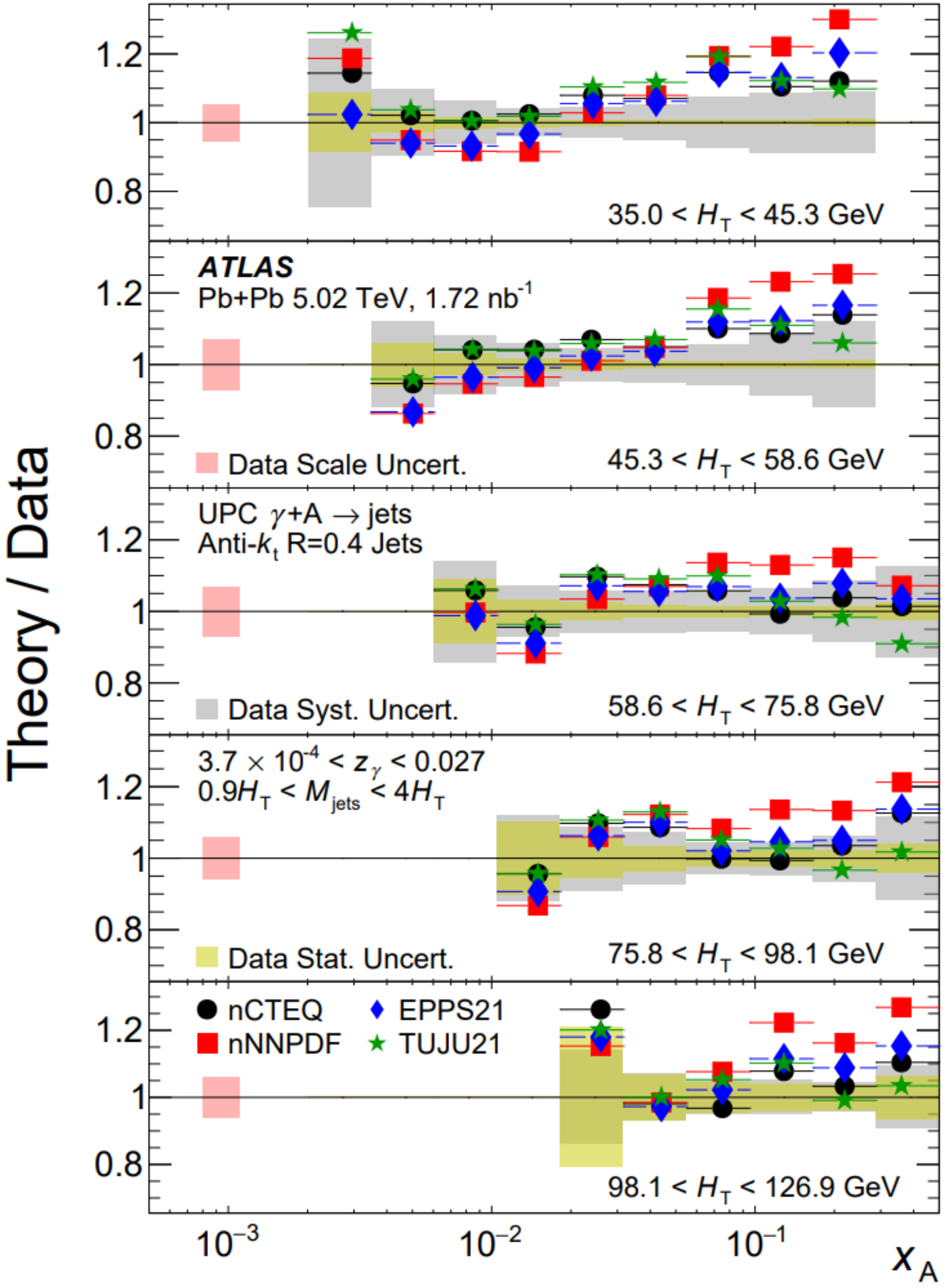

Conclusions

- This data can add a wide range of kinematic coverage to existing nPDF constraints.
  - All nPDF models have excess anti-shadowing, while nCTEQ15 WZ+SIH and TUJU21 agree with the shadowing observed in data at low H_T.
  - The full data tables allow for a complete treatment of correlated uncertainties, which will constrain nPDF effects even further.
- Photonuclear jet production was measured by ATLAS in 5.02 TeV Pb+Pb collisions with 2018 data.
  - This measurement extends to the lowest in jet p_T of any ATLAS measurement while maintaining systematic control.
    - This coverage is possible through a dedicated jet calibration produced specifically for jets in UPC.

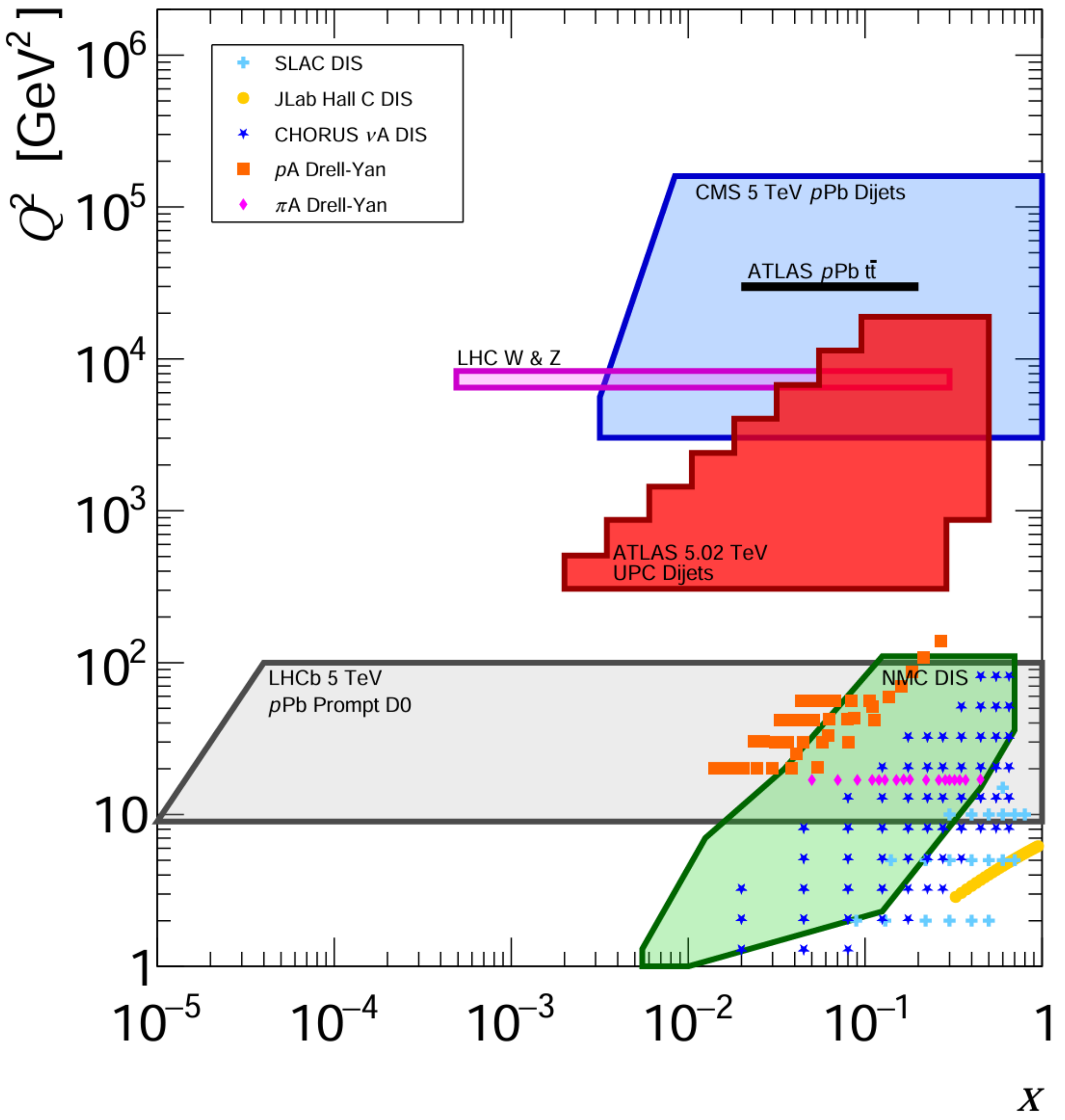

Figure inspired by arXiv:2112.12462

Conclusions

- This data can add a wide range of kinematic coverage to existing nPDF constraints.
  - All nPDF models have excess anti-shadowing, while nCTEQ15 WZ+SIH and TUJU21 agree with the shadowing observed in data at low H_T.
  - The full data tables allow for a complete treatment of correlated uncertainties, which will constrain nPDF effects even further.
- Photonuclear jet production was measured by ATLAS in 5.02 TeV Pb+Pb collisions with 2018 data.
  - This measurement extends to the lowest in jet p_T of any ATLAS measurement while maintaining systematic control.
    - This coverage is possible through a dedicated jet calibration produced specifically for jets in UPC.

These results are closely related to the early physics goals of the EIC!

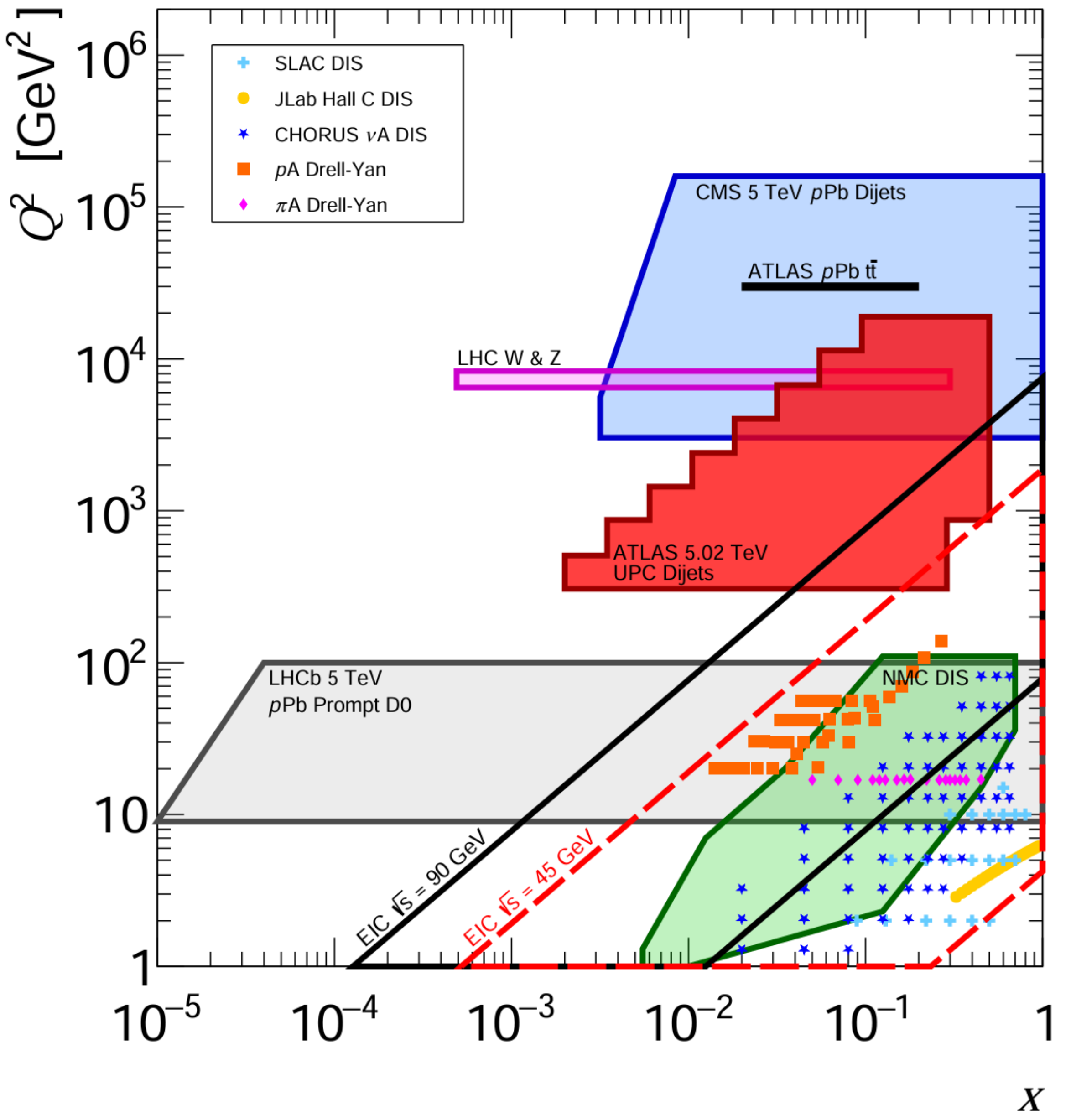

Figure inspired by arXiv:2112.12462

Backup

Photonuclear Jet Production

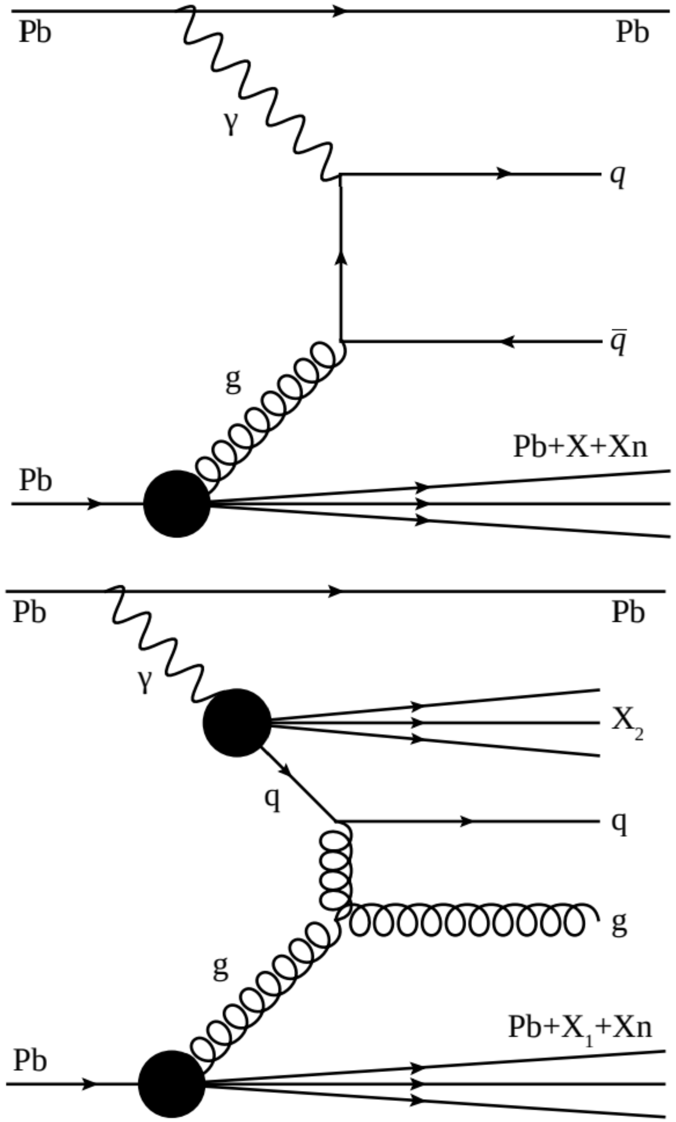

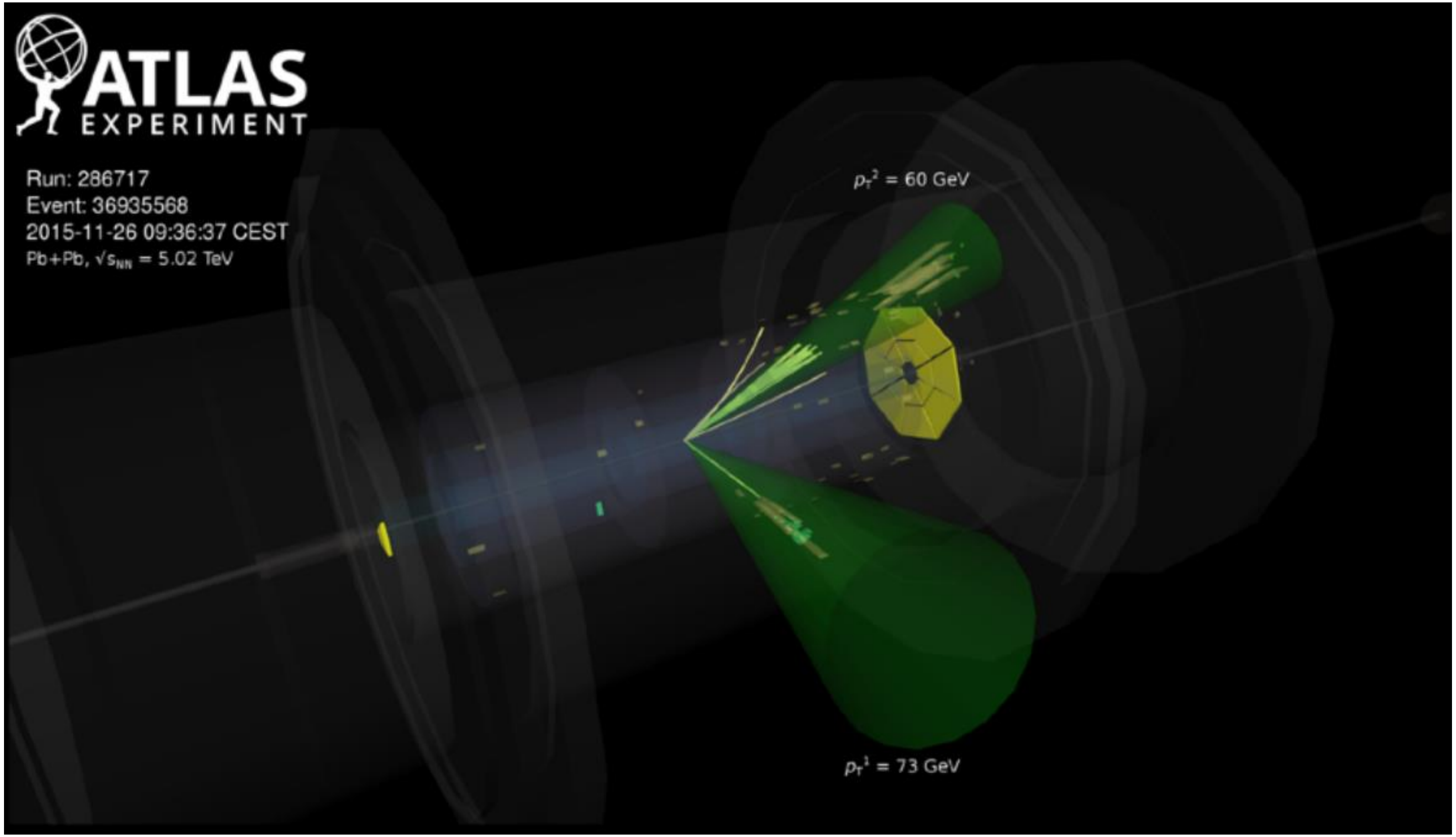

Jet Performance in MC

- The closure of the jet energy scale in MC is excellent, with <0.5% non-closures over the majority of the detector.
  - The closure performs slightly worse and the resolution is larger in the 3.2-3.5 region.
    - This region corresponds to a transition in the ATLAS calorimeter.
- The shape of the JER at very low p_T arises from particle flow within the inner detector acceptance.

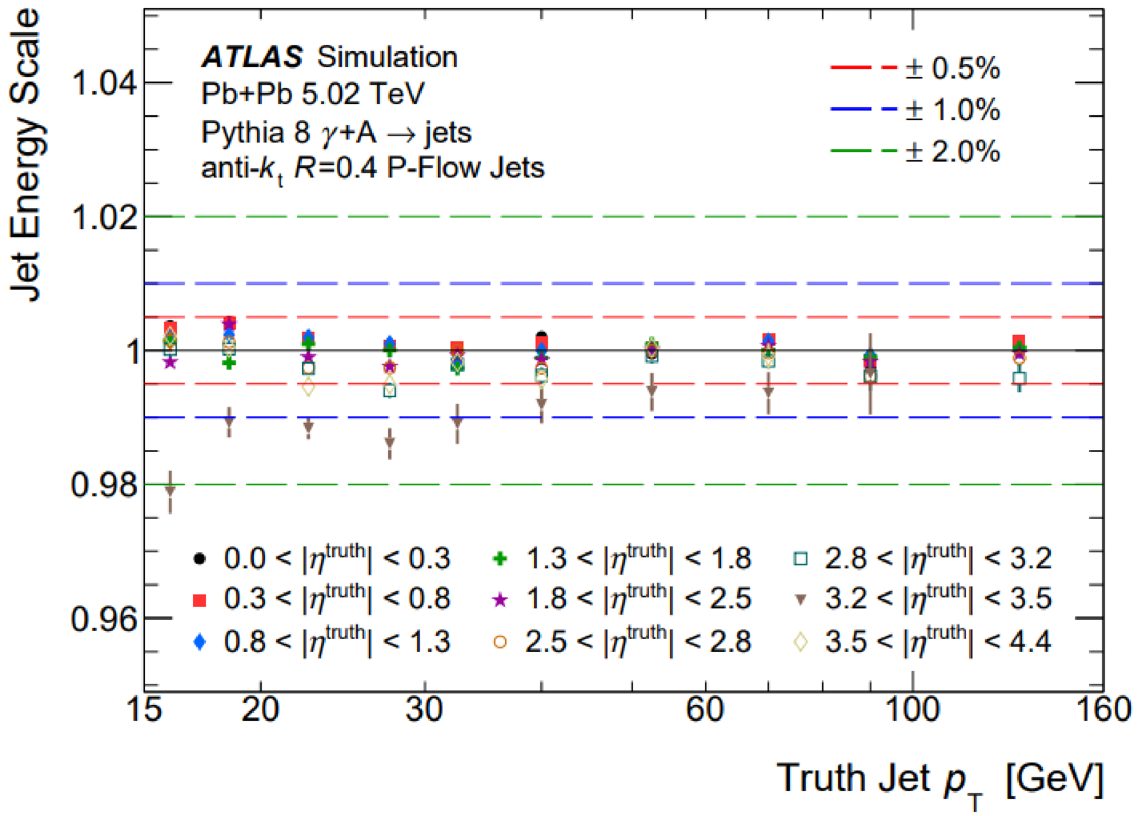

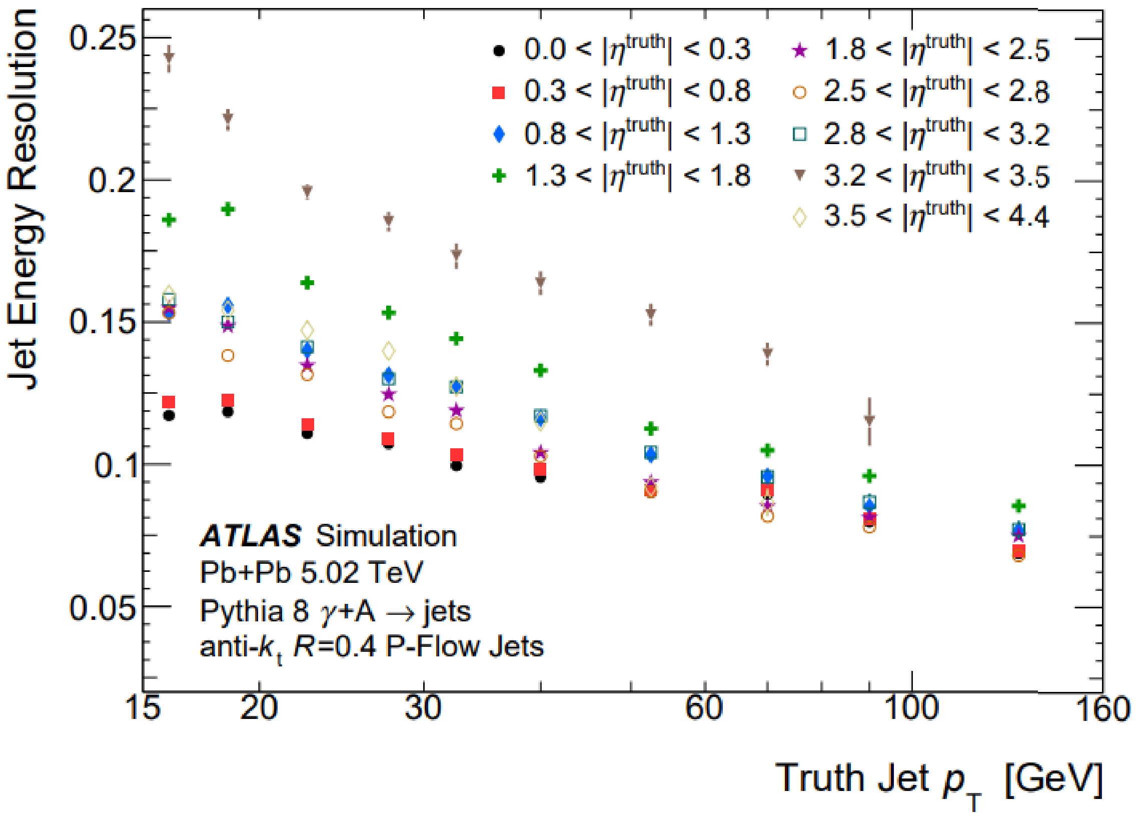

Jet Performance in Data

- The jet response in data is constrained through two studies:
  - Z+jet balance to constrain the absolute energy scale at mid-rapidity
  - Dijet balance to constrain the relative energy scale between regions of the detector
- Uncertainties are also assessed due to jet flavor composition and response.

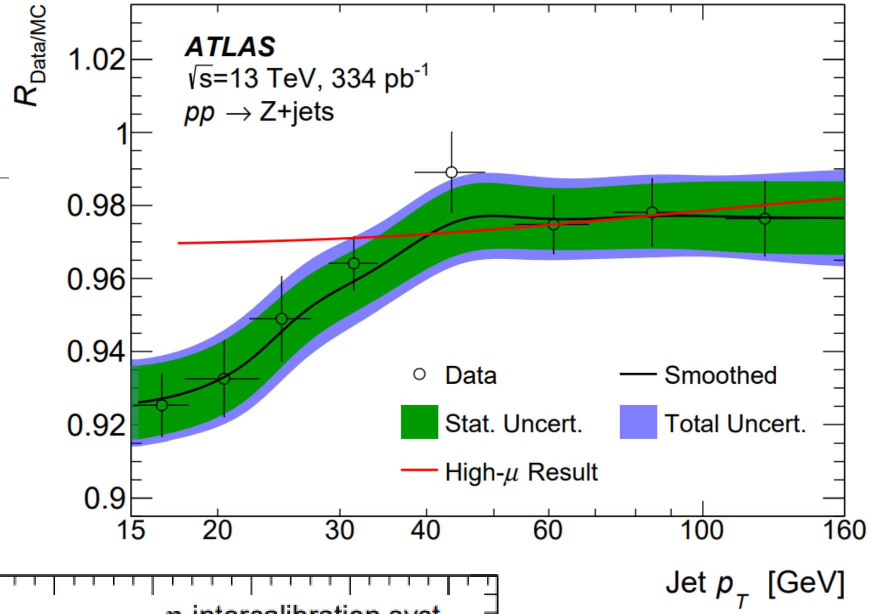

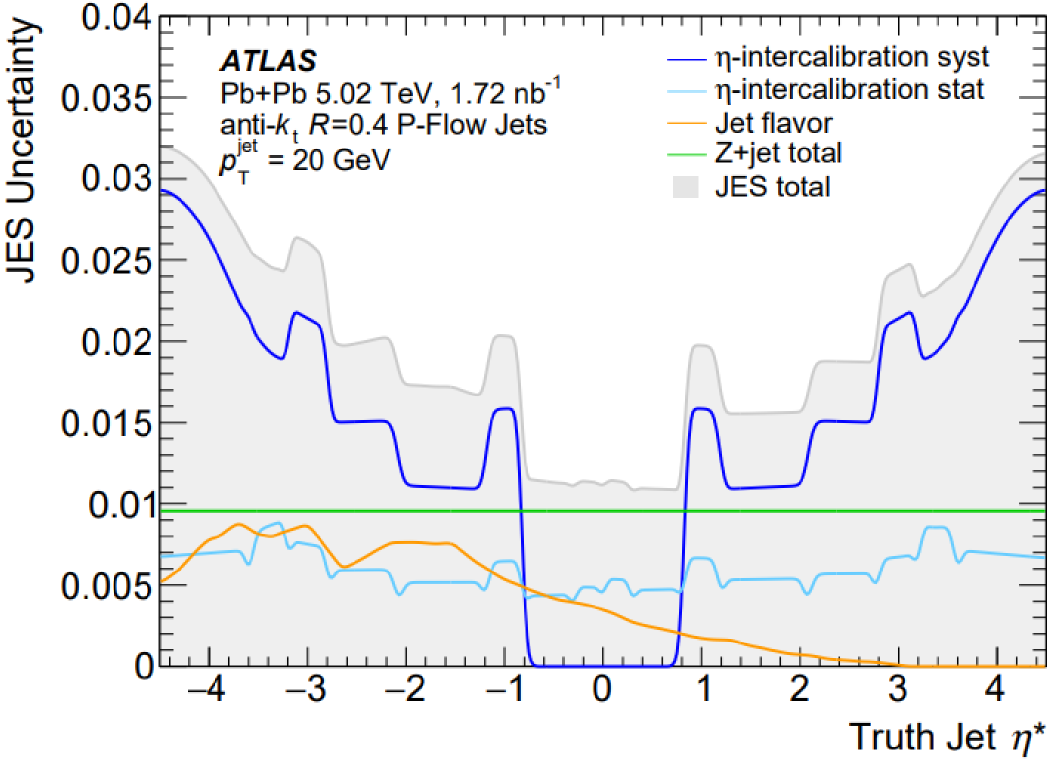

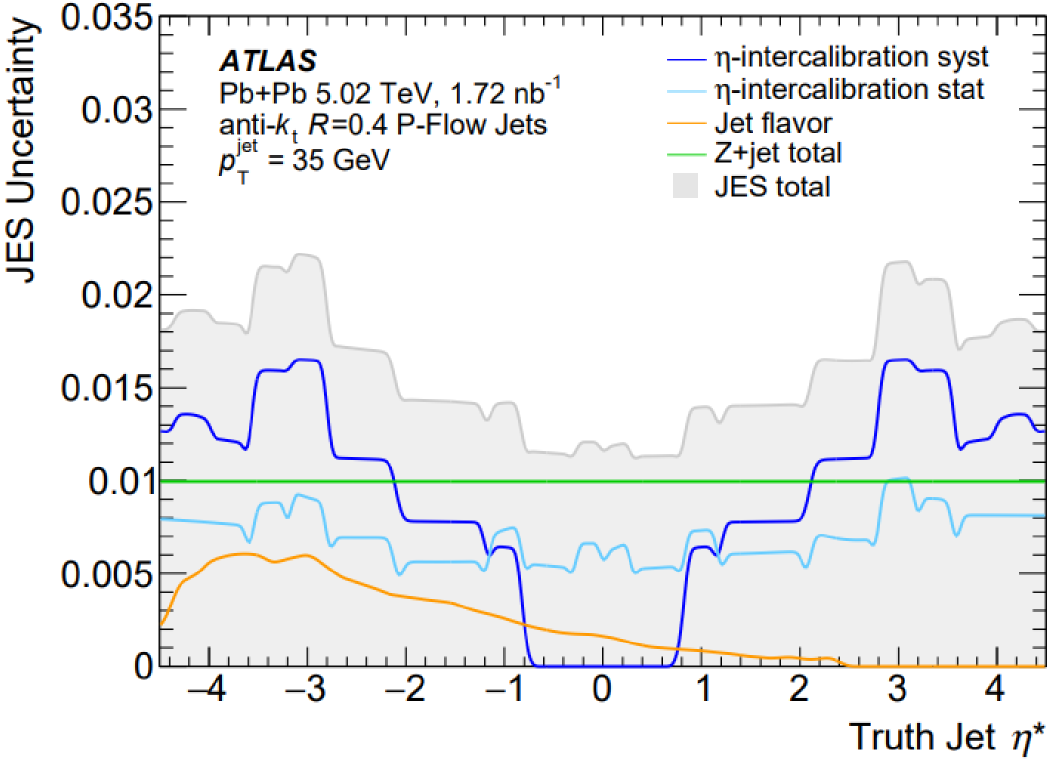

Nucleus-Going Gap Requirements

- Nucleus-going gap selections are also tuned to remove backgrounds from "reverse" events and photo-diffractive jet production.

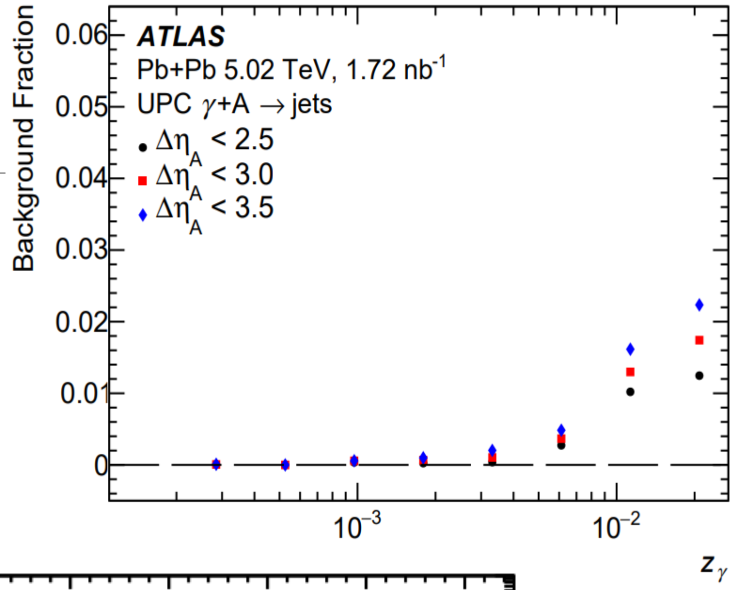

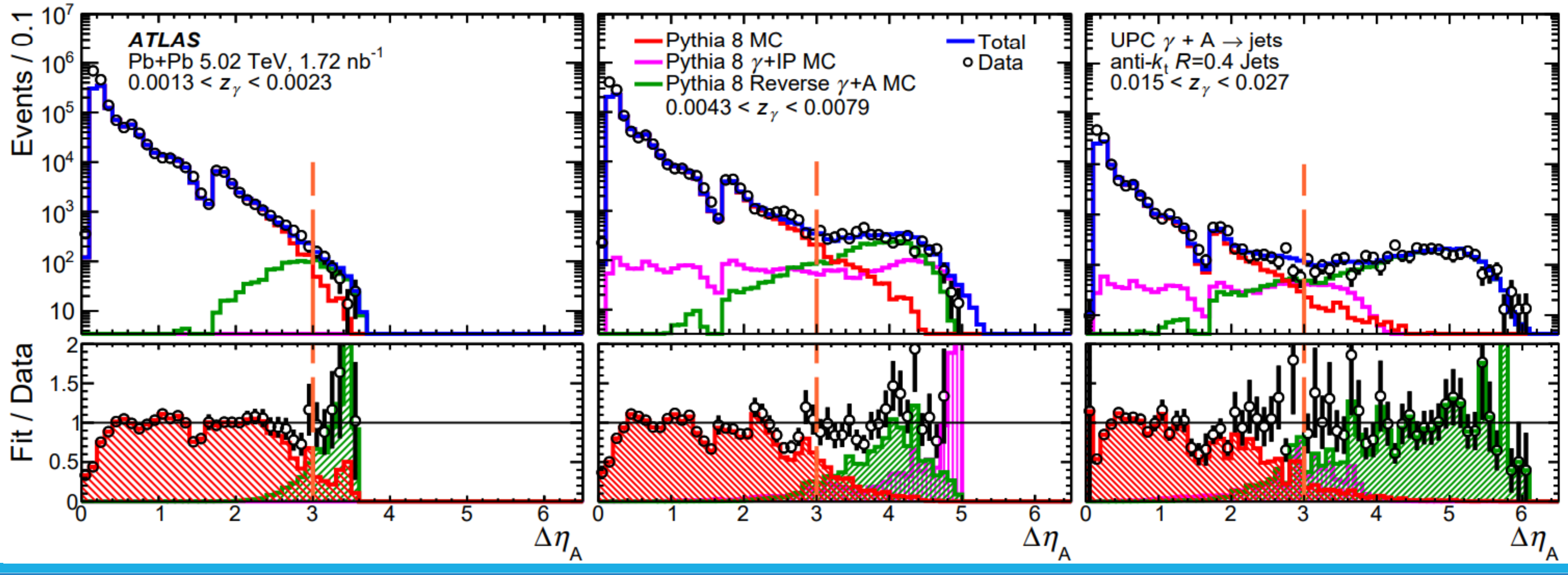

Acceptance and Observables

Jet	Event
$p_T^{jet} > 15$ GeV $\lvert\eta^{jet}\rvert < 4.4$	ZDC $0nXn$: $E_{0n} < 1$ TeV and $E_{Xn} > 1$ TeV $N_{jet} \geq 2$ $0.9H_T < m_{jets} < 4H_T$ $\sum_\gamma \Delta\eta > 2.5$, $\Delta\eta_A < 3$, and $\sum \Delta\eta < 9$

$$H_T = \sum_i p_T^i$$

$$x_A = \frac{M_{jets}e^{-y_{jets}}}{\sqrt{s_{NN}}}$$

$$z_\gamma = \frac{M_{jets}e^{+y_{jets}}}{\sqrt{s_{NN}}}$$

Cross-sections are measured and unfolded in H_T, x_A, and z_γ.

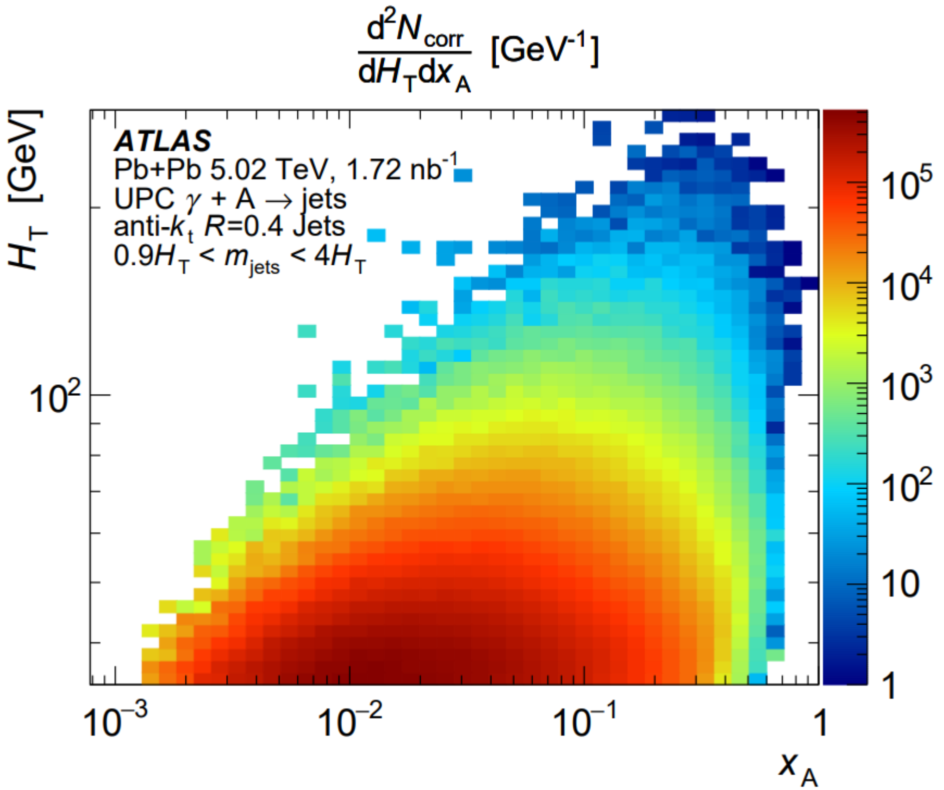

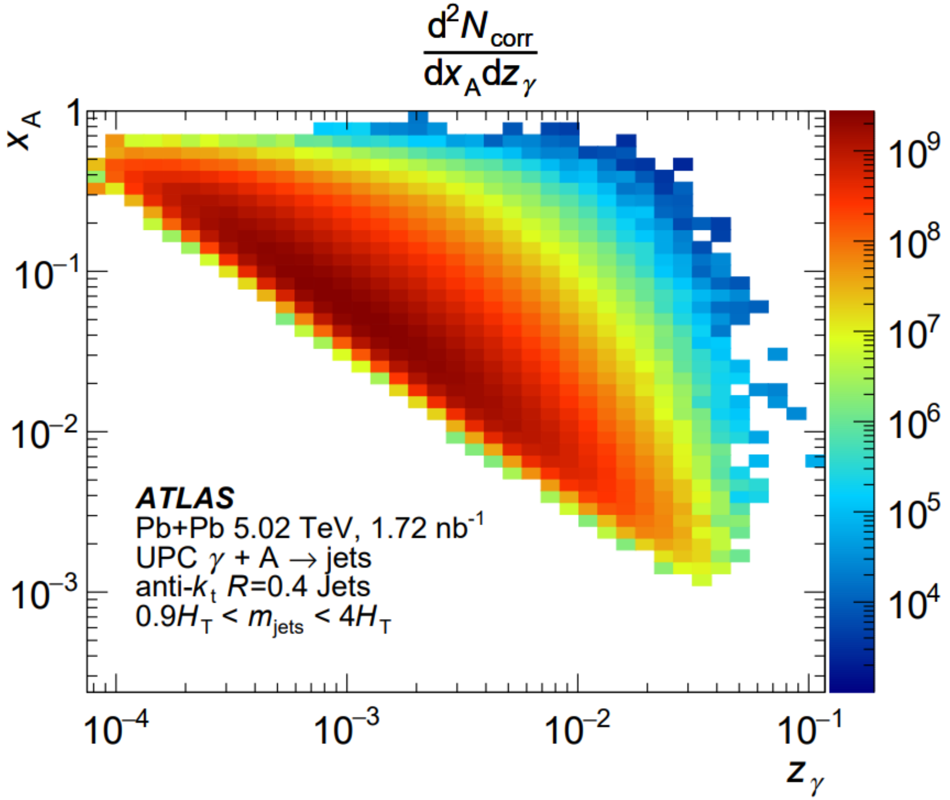

Data-MC Comparisons

$$m_{\text{jets}} \equiv \left[\left(\sum_i E_i\right)^2 - \left|\sum_i \vec{p}_i\right|^2\right]^{1/2}$$

$$y_{\text{jets}} \equiv \frac{1}{2}\ln\left(\frac{\sum_i E_i + \sum_i p^*_{zi}}{\sum_i E_i - \sum_i p^*_{zi}}\right)$$

Jet	Event
$p_{\mathrm{T}}^{\text{jet}} > 15$ GeV $\lvert\eta^{\text{jet}}\rvert < 4.4$	ZDC $0nXn$: $E_{0n} < 1$ TeV and $E_{Xn} > 1$ TeV $N_{\text{jet}} \geq 2$ $0.9H_{\mathrm{T}} < m_{\text{jets}} < 4H_{\mathrm{T}}$ $\sum_{\gamma}\Delta\eta > 2.5$, $\Delta\eta_A < 3$, and $\sum\Delta\eta < 9$

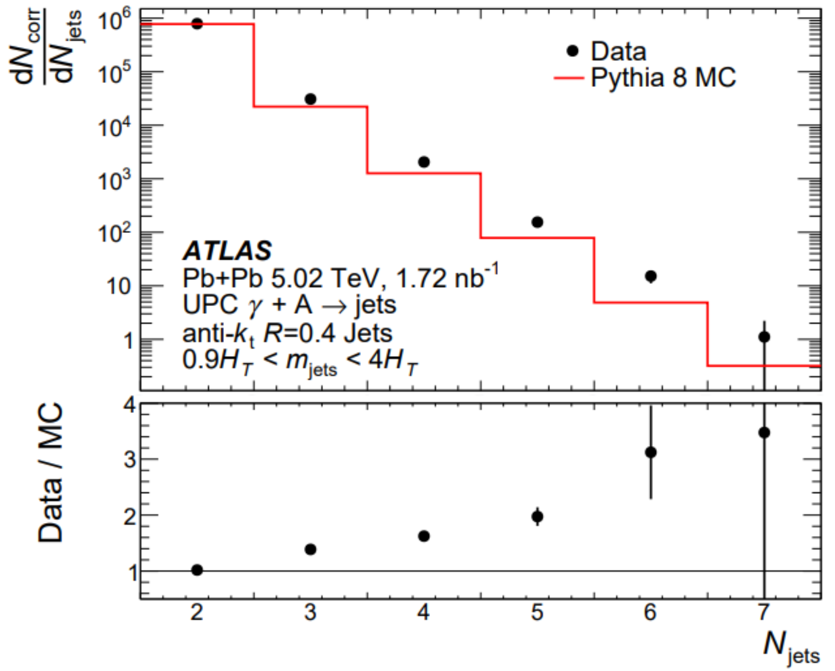

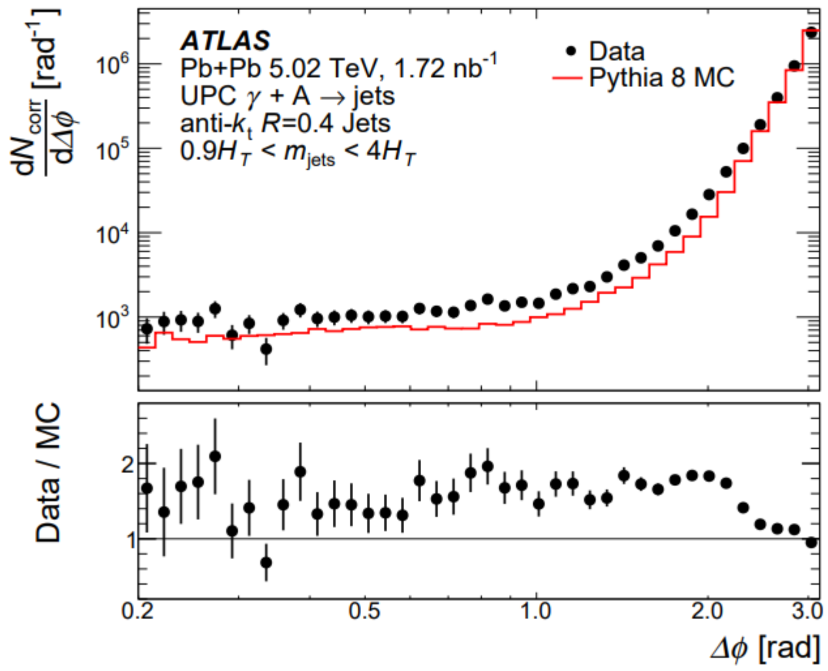

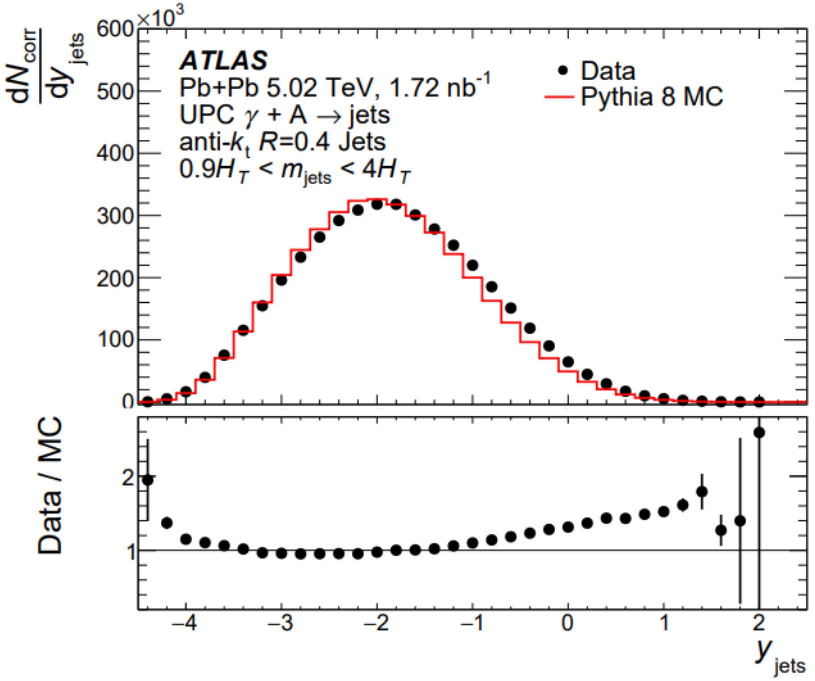

The Measured Photon Flux

- The distribution of z_γ values for large x_A in bins of H_T (right) demonstrates the measured photon flux.
  - Disagreements appear to arise at low z_γ and low H_T, which could arise due to:
    - Photon flux modeling
    - NLO corrections the LO+PS Pythia calculation

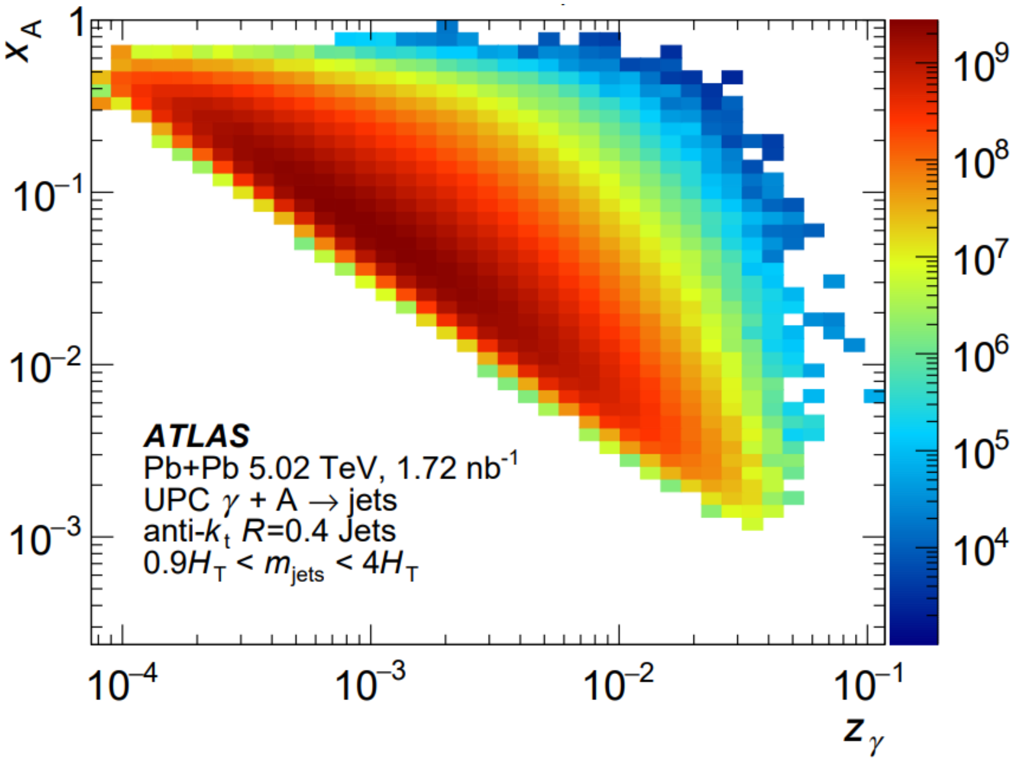

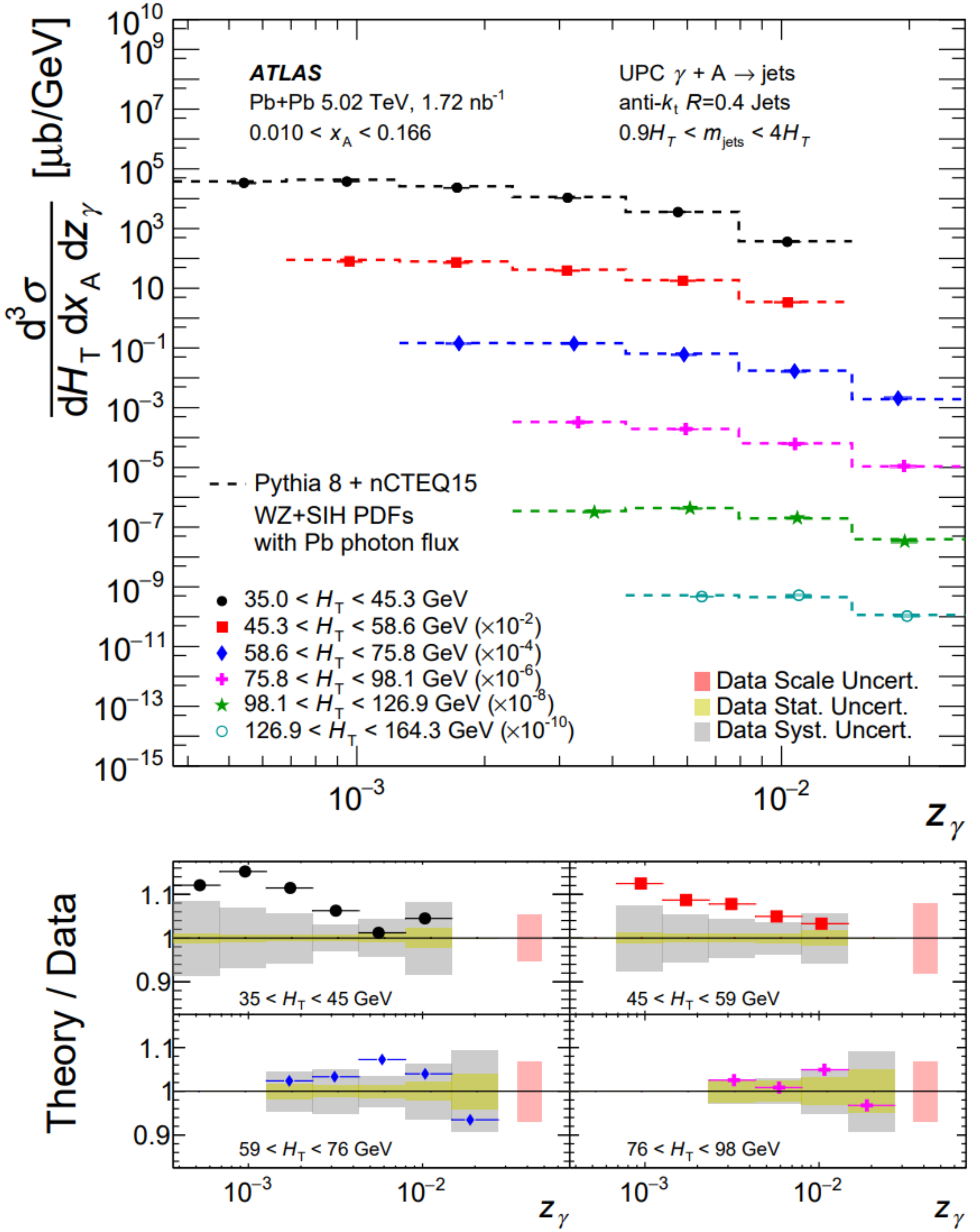

Correlated Uncertainties and nPDF Effects

- Correlated systematic uncertainties are treated in the following figures are represented by separating out the “scale” fully correlated across all points.

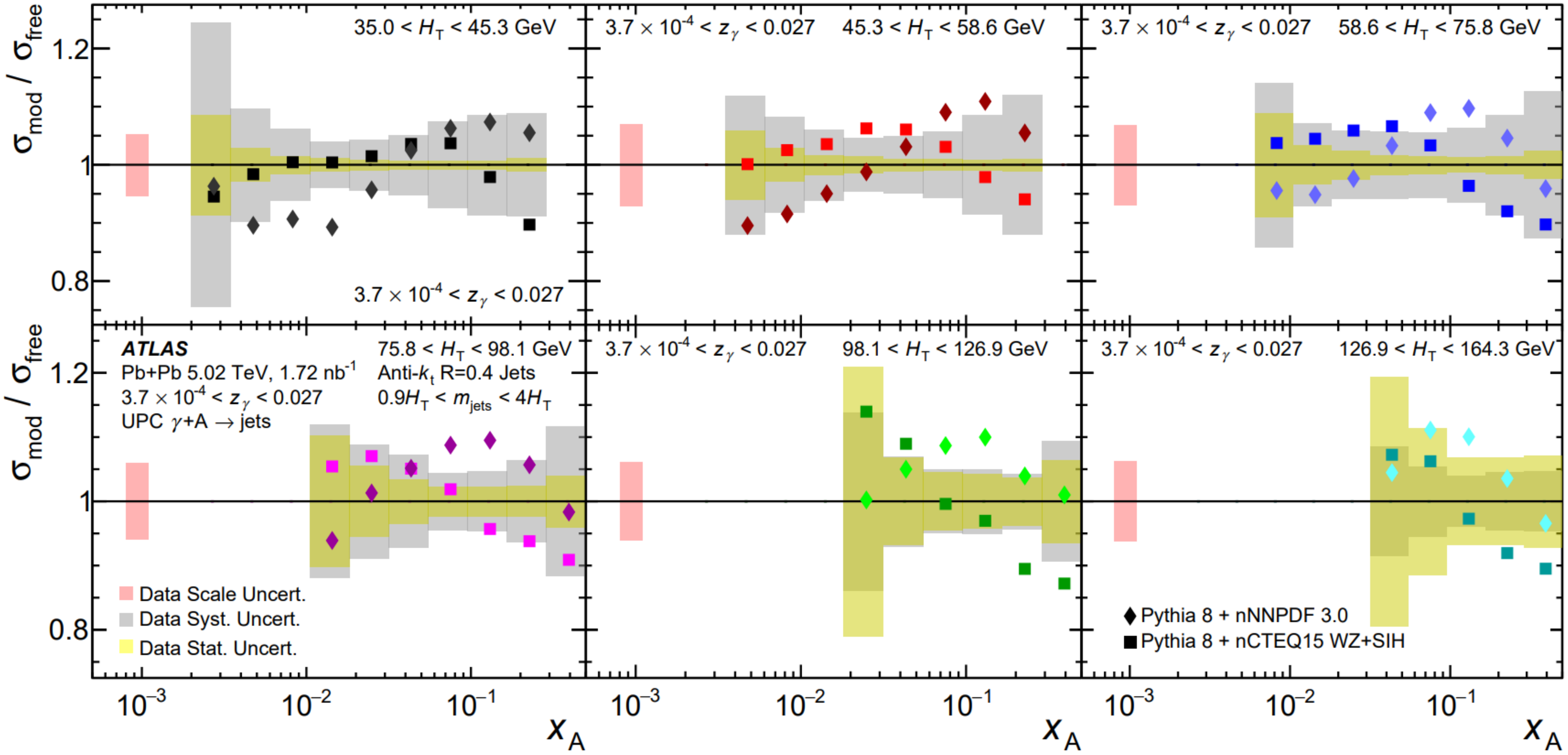

Cross-Sections vs. H_T

- For a given slice in x_A, the dependence on H_T can help to:
  - Separate correlated systematic uncertainties
  - Understand the variation of nPDF modification with Q^2

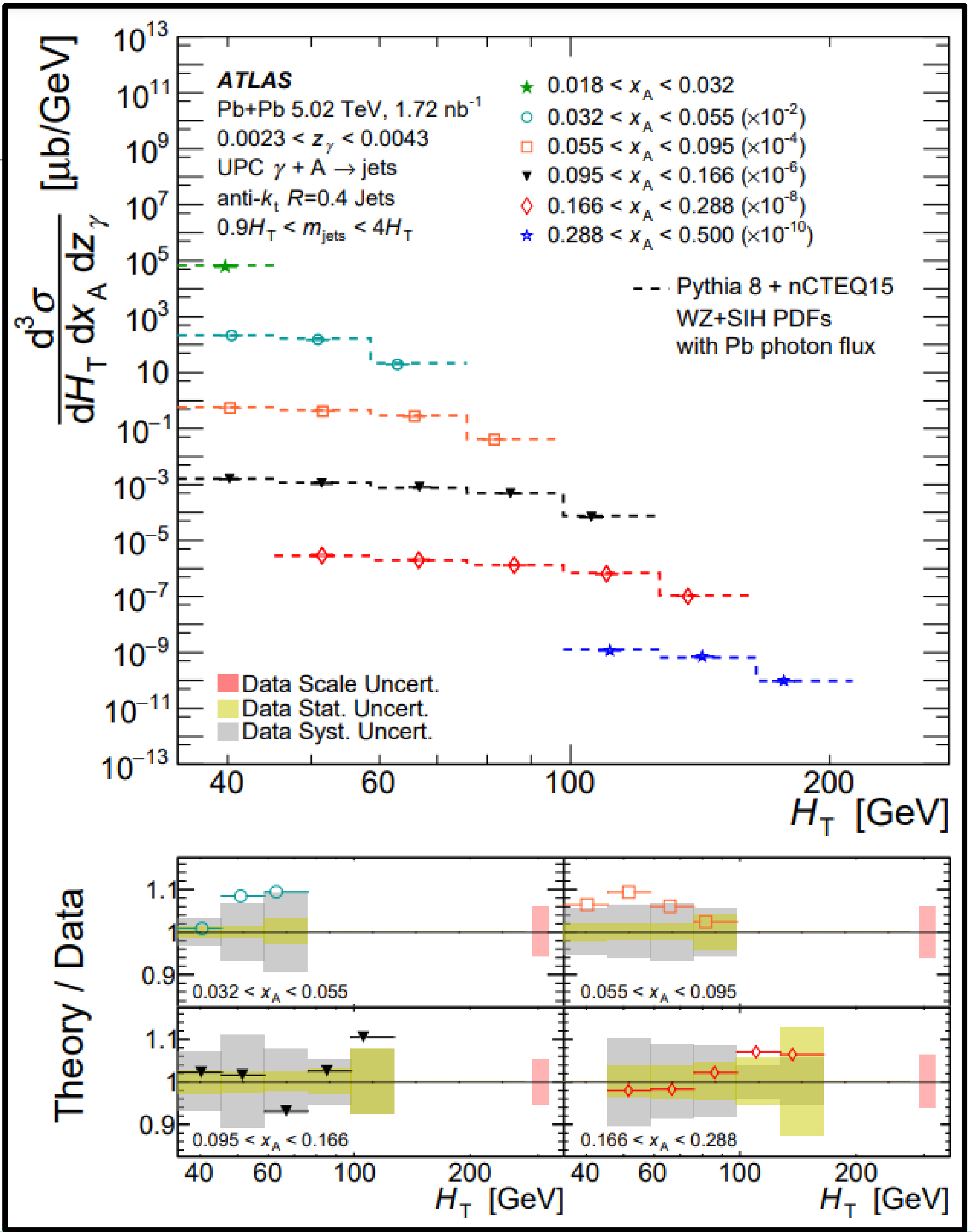

Cross-Sections vs. H_T

- For a given slice in x_A, the dependence on H_T can help to:
  - Separate correlated systematic uncertainties
  - Understand the variation of nPDF modification with Q^2

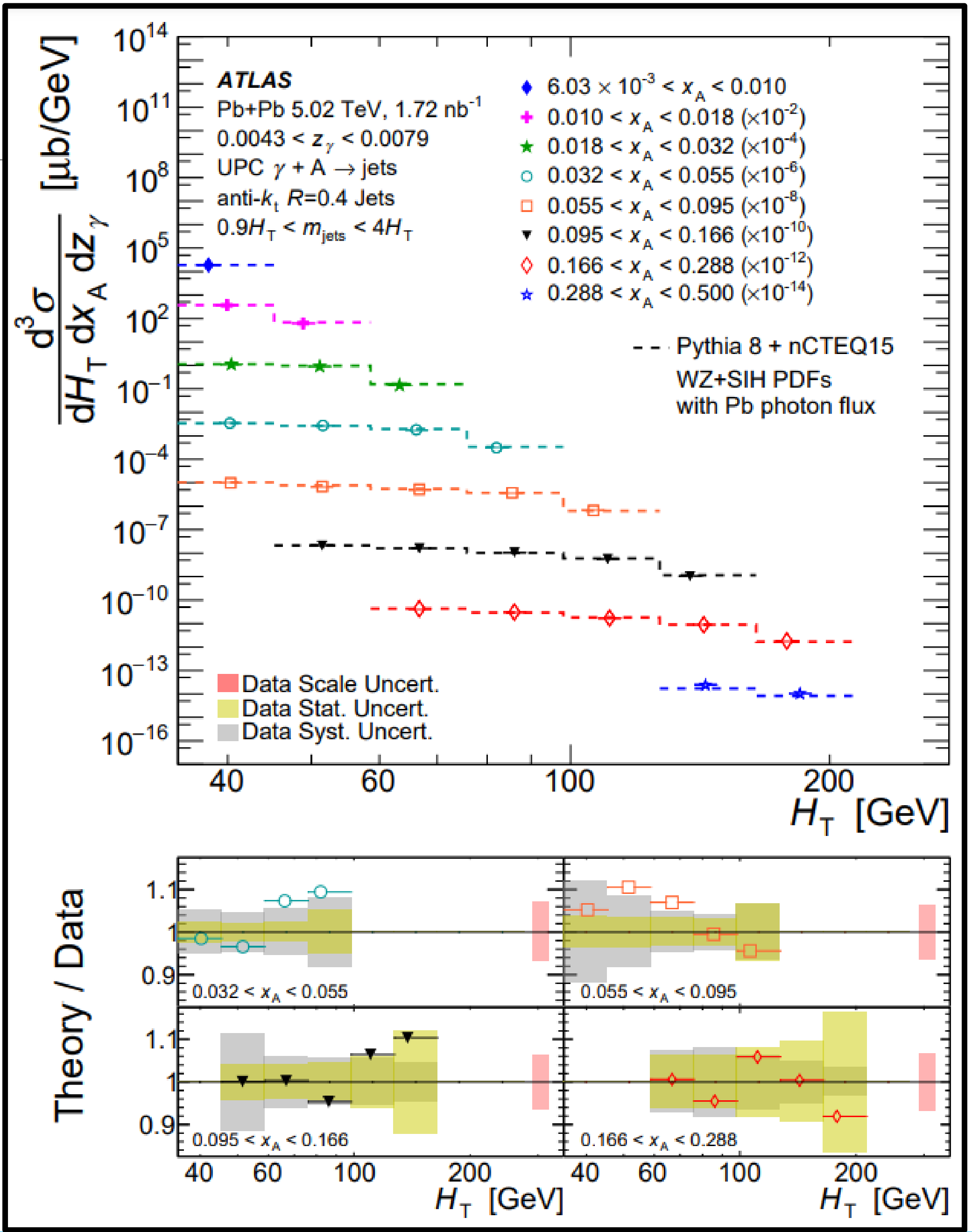

Cross-Sections vs. H_T

- For a given slice in x_A, the dependence on H_T can help to:
  - Separate correlated systematic uncertainties
  - Understand the variation of nPDF modification with Q^2

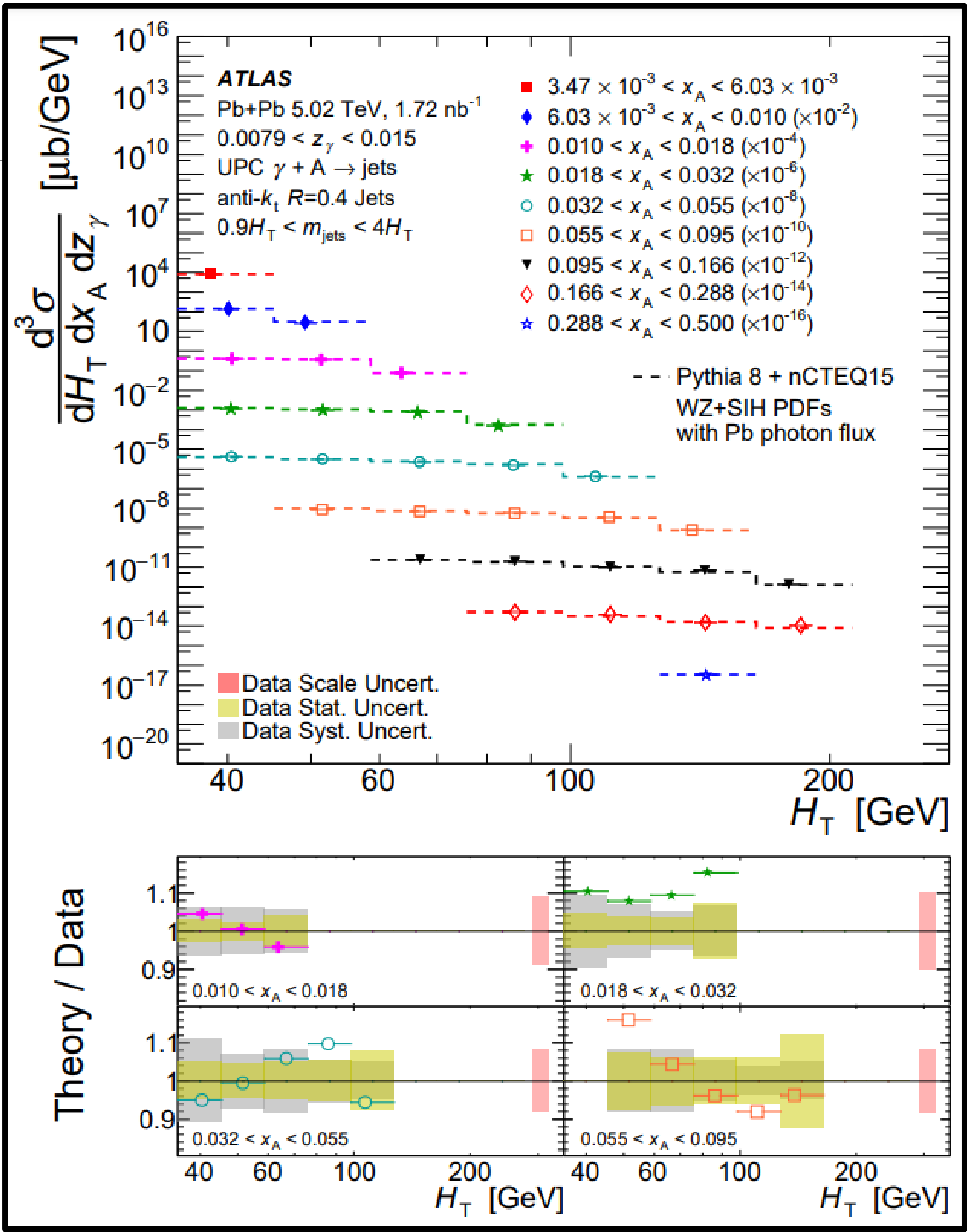

Cross-Sections vs. H_T

- For a given slice in x_A, the dependence on H_T can help to:
  - Separate correlated systematic uncertainties
  - Understand the variation of nPDF modification with Q^2

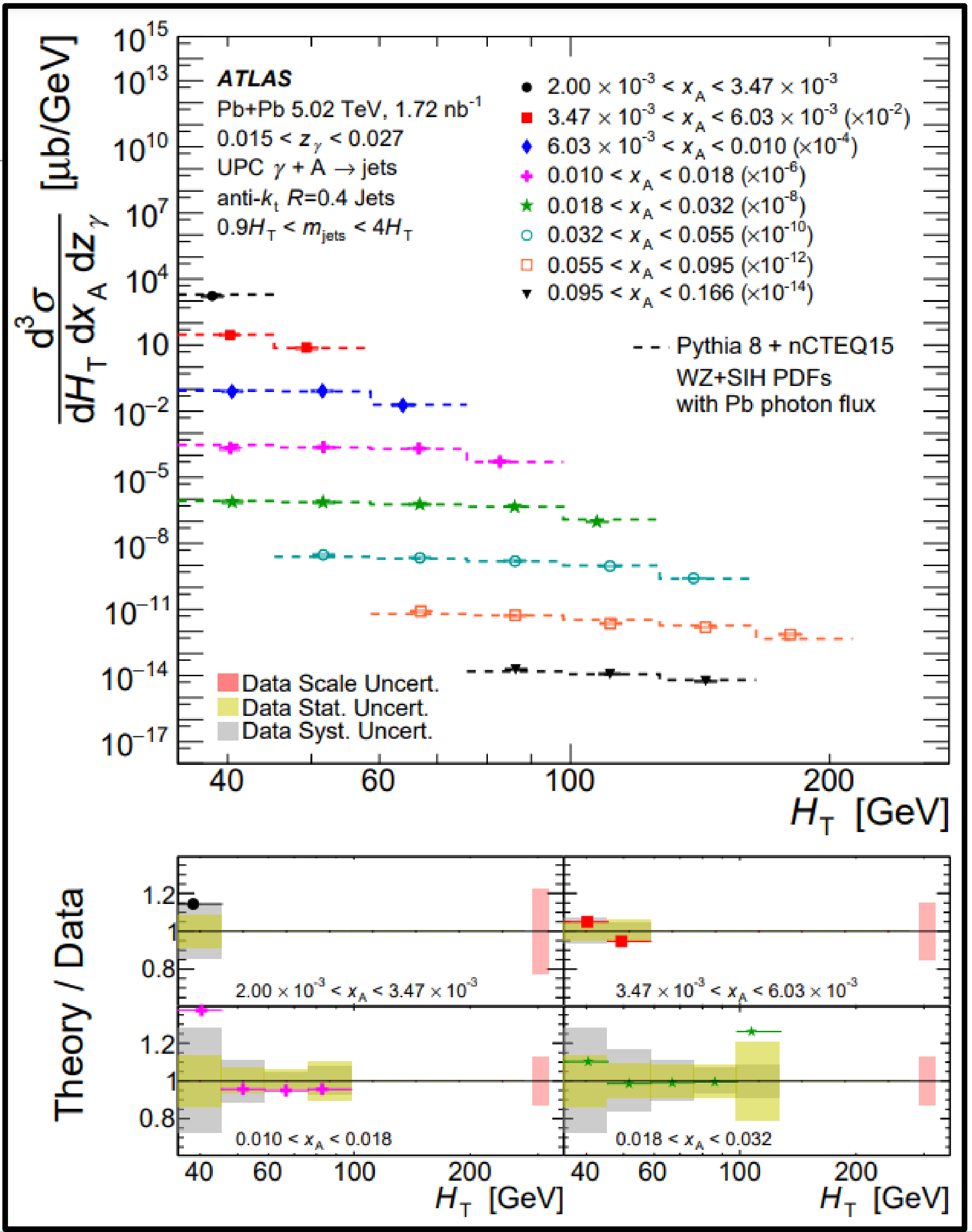

Cross-Sections vs. H_T

- For a given slice in x_A, the dependence on H_T can help to:
  - Separate correlated systematic uncertainties
  - Understand the variation of nPDF modification with Q^2

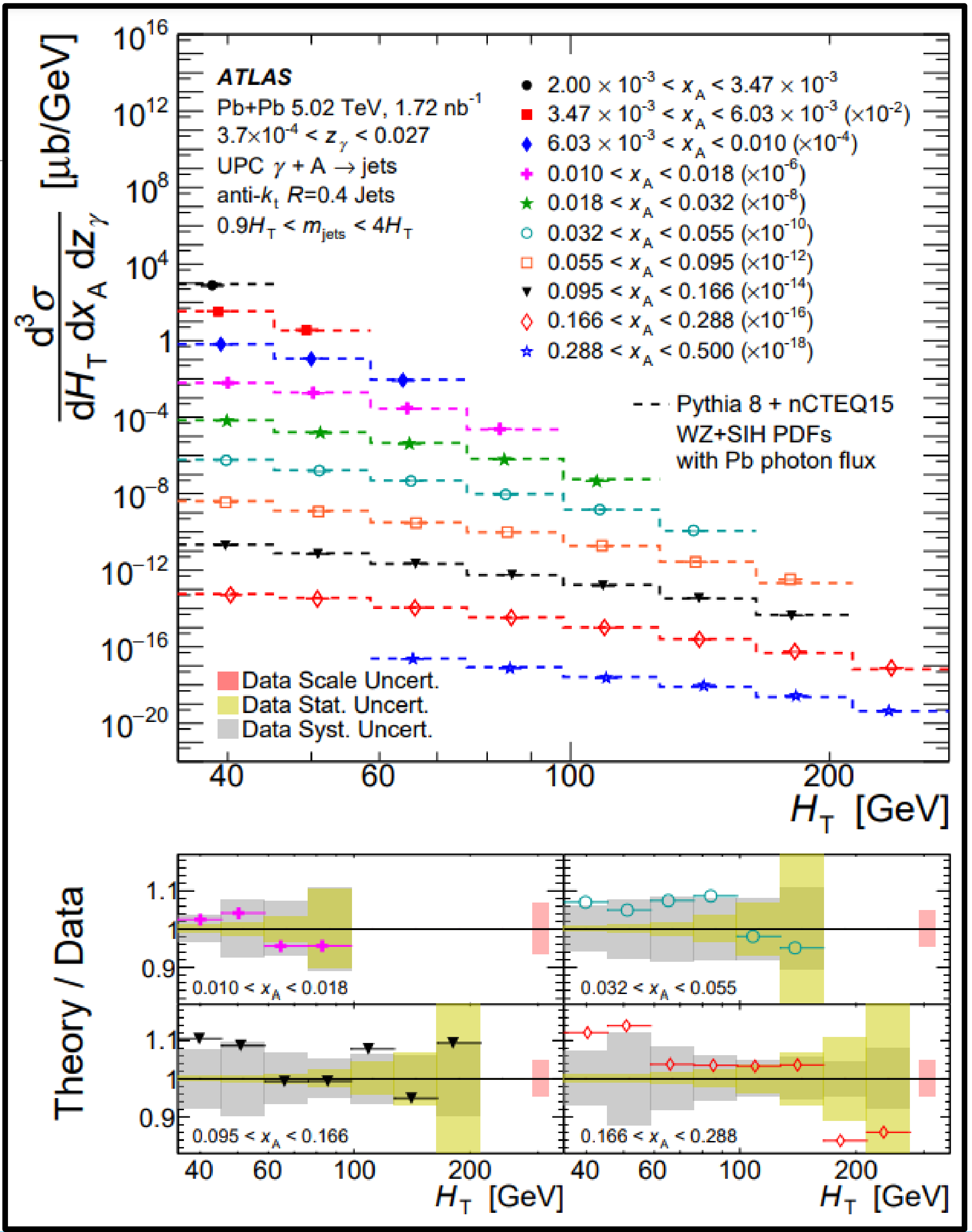

Jet System Kinematics

- Unfolded jet cross-sections are also produced in a different variable set, in terms of the jet system kinematics.
- Results are broadly consistent with the hard-scattering kinematics.
- At low H_T, the cross-section is over-predicted in the nucleus-going direction but quite consistent in the photon-going direction.

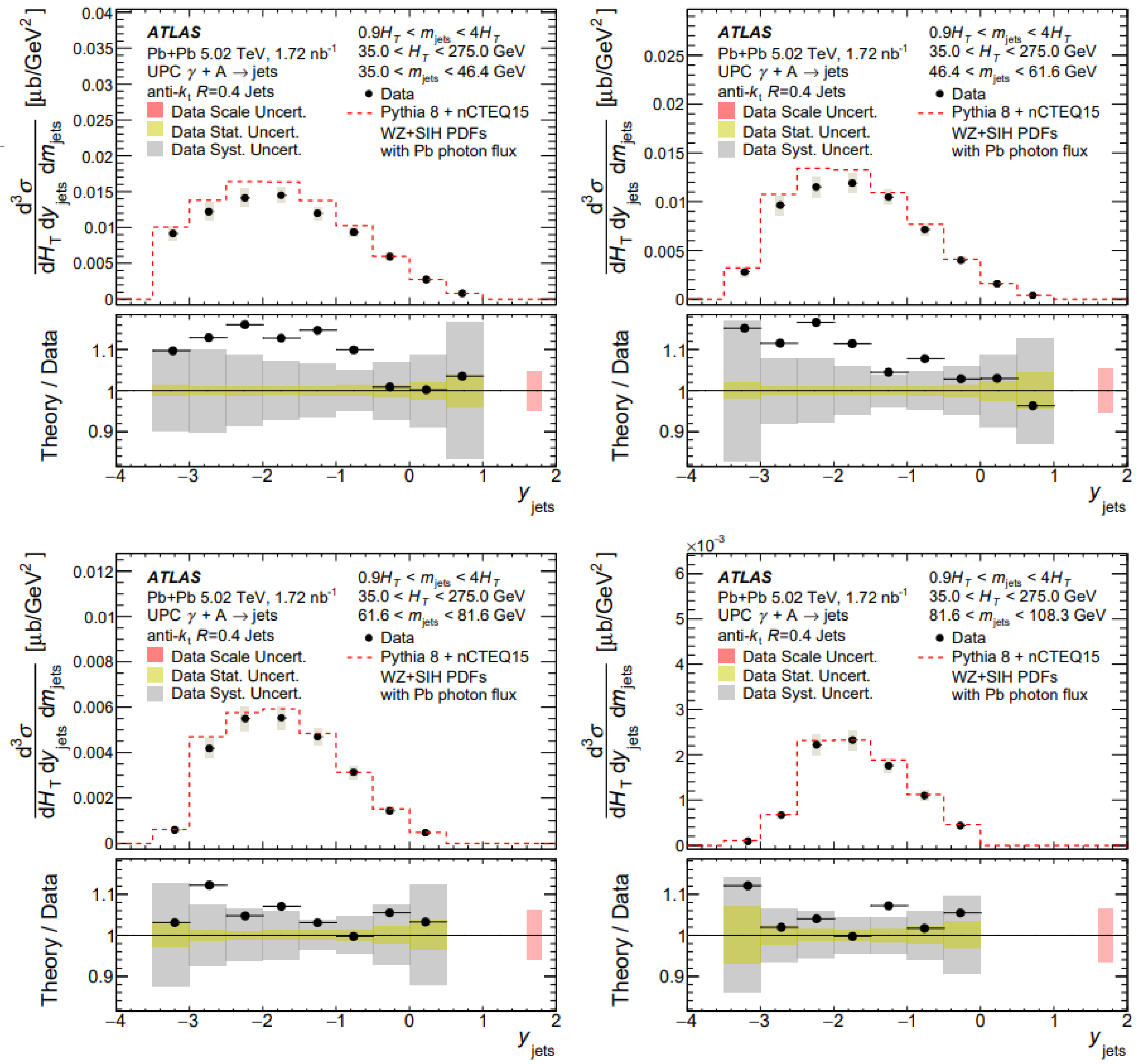

Jet System Kinematics

- Unfolded jet cross-sections are also produced in a different variable set, in terms of the jet system kinematics.
- Results are broadly consistent with the hard-scattering kinematics.
- At low H_T, the cross-section is over-predicted in the nucleus-going direction but quite consistent in the photon-going direction.
- The mass-dependence demonstrates that inconsistencies are concentrated at small mass, but the higher-mass bins are well-predicted.

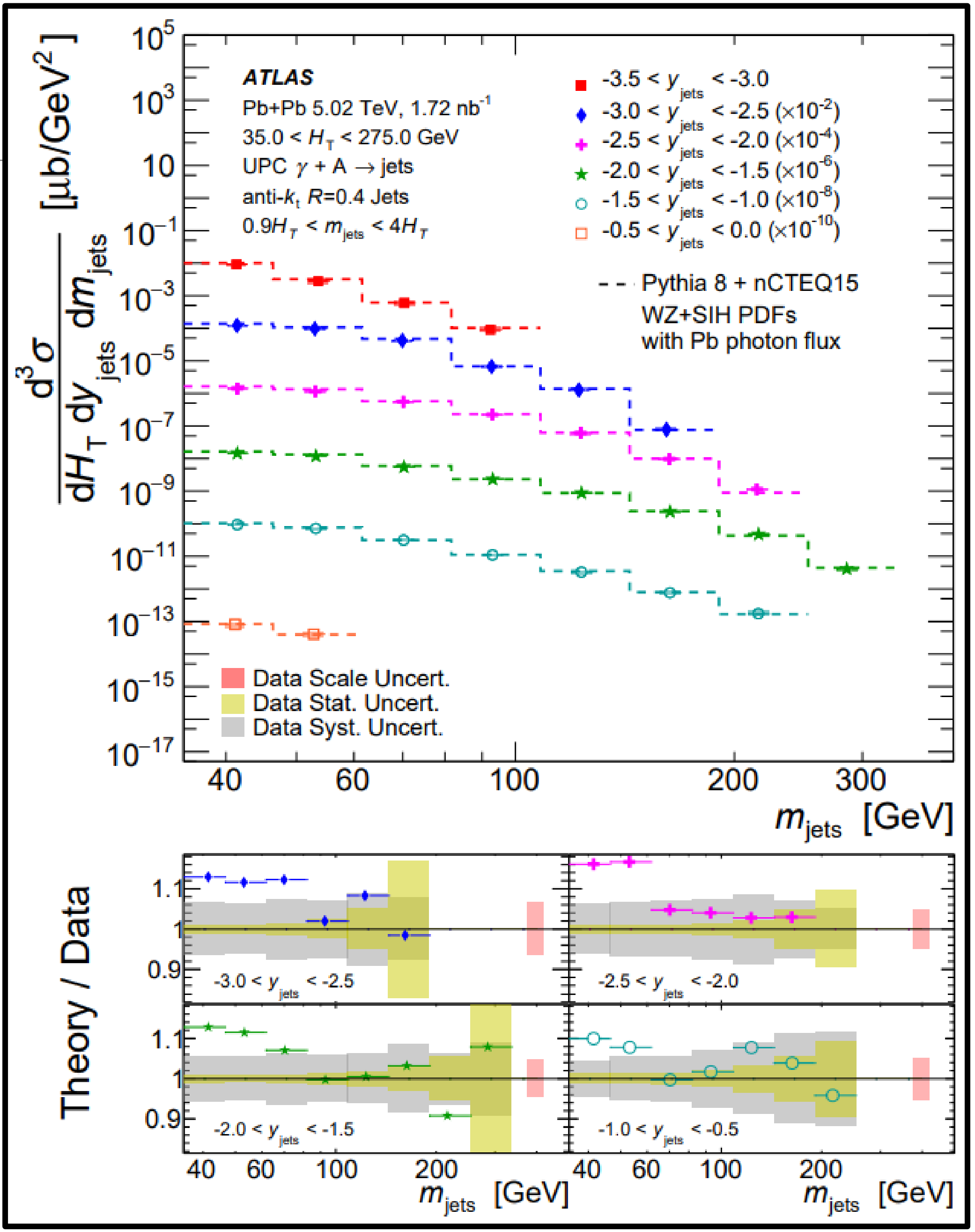

Bin Acceptance

- Bins are only reported if the measurement acceptance is high enough in that region.
- The acceptance is limited due to the mapping of single-jet selections onto the 3D phase space.
- Selection effects also shift bin means, which we account for.

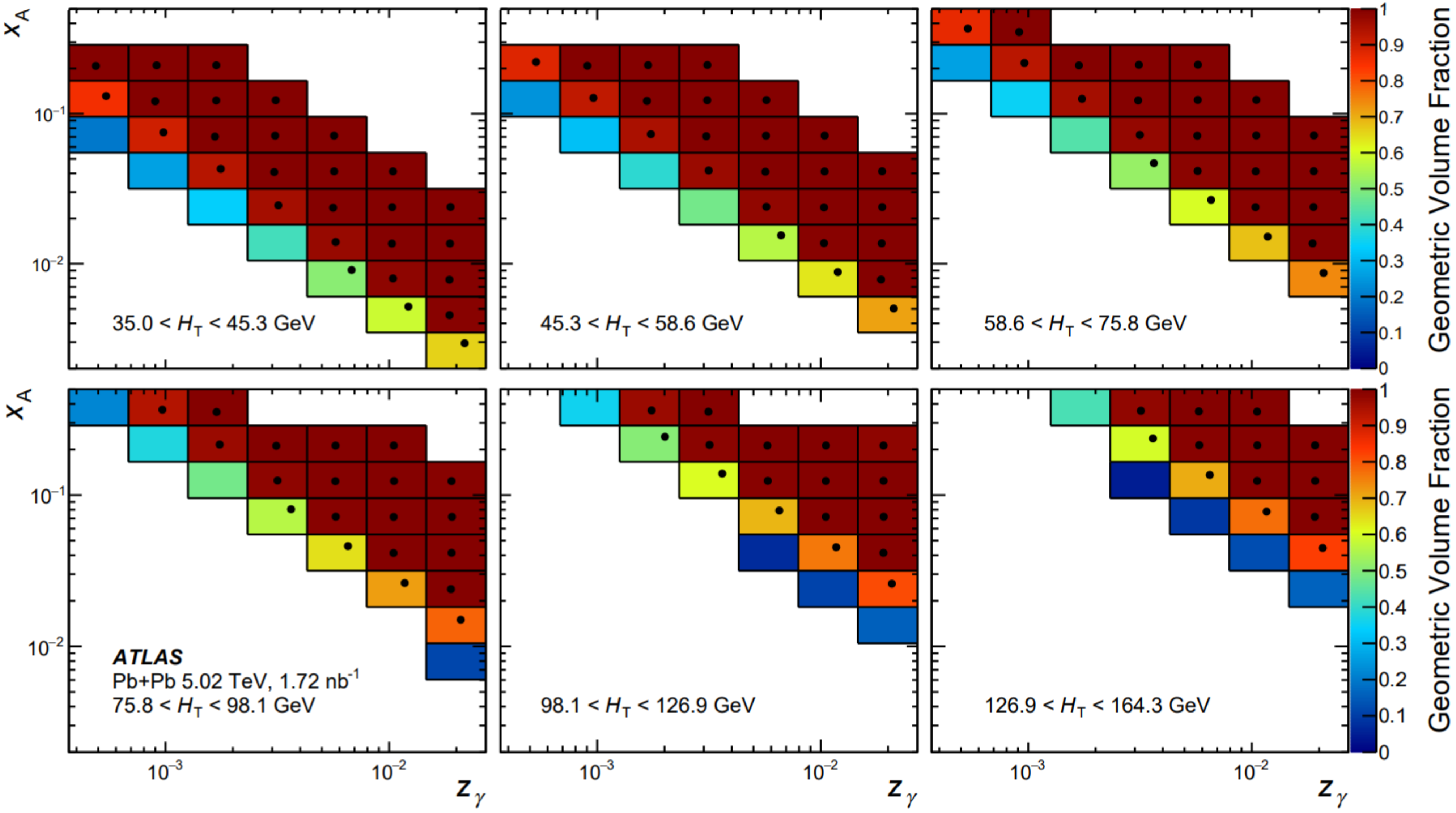

nPDF Comparisons

- The approach of each nPDF fit to describing the data is different, making it difficult to ascribe differences to only the datasets included:
  - nCTEQ and TUJU fit the nPDF independent of the free proton PDF. TUJU restricts to NNLO calculations.
  - EPPS directly fits the modification relative to CT18A.
  - nNNPDF fits using a neural network approach.

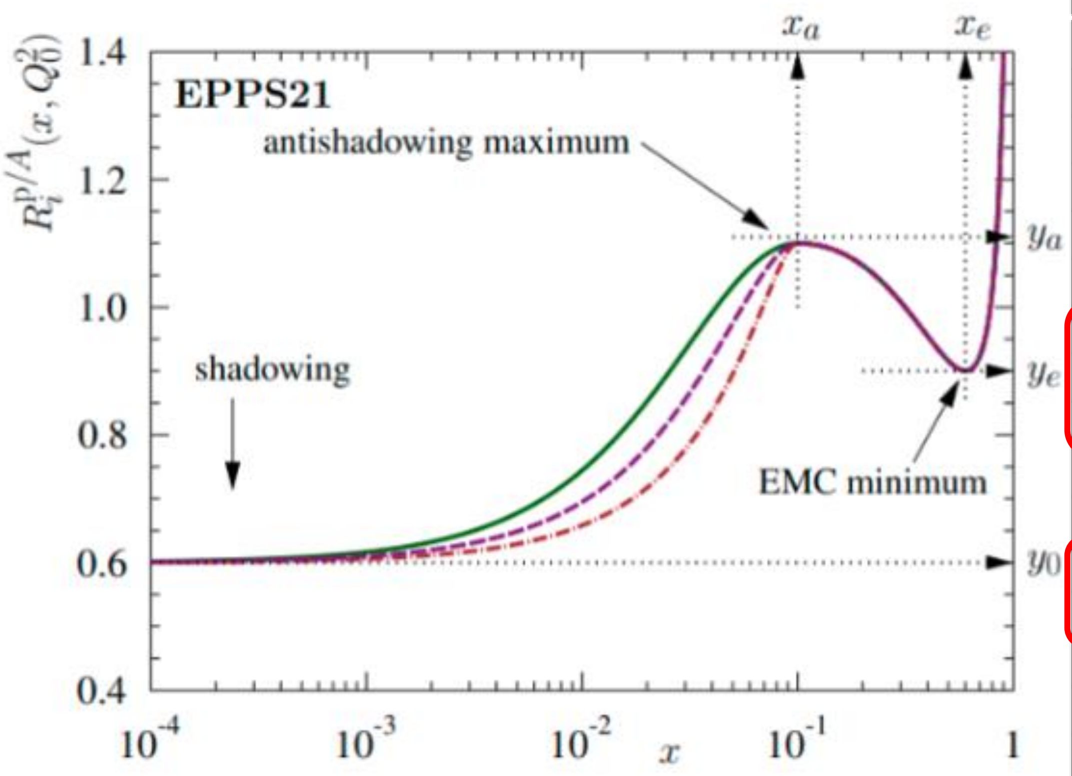

Dataset Description	nCTEQ15WZ+SIH	EPPS21	nNNPDF 3.0	TUJU21
SLAC/FNAL/CERN/Hermes DIS	✓	✓	✓	✓
JLab CLAS+Hall C eA DIS	✓	✓		
CHORUS/CDHSW νA DIS	✓	✓	✓	✓
NuTeV/CCFR νA DIS	✓		✓	
FNAL pA Drell-Yan	✓	✓	✓	
FNAL/NA3/NA10 πA Drell-Yan		✓		
STAR+PHENIX Inclusive π^0	✓	✓		
STAR+PHENIX η, $\pi^\pm$	✓			
PHENIX $K^\pm$	✓			
LHC Z^0 Bosons	✓	✓	✓	✓
CMS+ALICE $W^\pm$ Bosons	✓	✓	✓	✓
ALICE π^0, η, $\pi^\pm$, $K^\pm$	✓			
CMS pPb Dijets		✓	✓	
ATLAS pPb Prompt Photons			✓	
LHCb pPb Prompt D^0	✓	✓	✓	
ALICE pPb Prompt D^0	✓			